energy&fuels

Deep Eutectic Solvents: Physicochemical Properties and Gas Separation Applications

Gregorio García,[†] Santiago Aparicio,*,[†] Ruh Ullah,[‡] and Mert Atilhan*,[‡]

[†]Department of Chemistry, University of Burgos, 09001 Burgos, Spain
[‡]Department of Chemical Engineering, Qatar University, P.O. Box 2713, Doha, Qatar

S *Supporting Information*

ABSTRACT: Sustainable technologies applied to energy-related applications should develop a pivotal role in the next decades. In particular, carbon dioxide capture from flue gases emitted by fossil-fueled power plants should play a pivotal role in controlling and reducing the greenhouse effect. Therefore, the development of new materials for carbon capture purposes has merged as central research line, for which many alternatives have been proposed. Ionic liquids (ILs) have emerged as one of the most promising choices for carbon capture, but in spite of their promising properties, some serious drawbacks have also appeared. Deep eutectic solvents (DESs) have recently been considered as alternatives to ILs that maintain most of their relevant properties, such as task-specific character, and at the same time avoid some of their problems, mainly from economic and environmental viewpoints. DES production from low-cost and natural sources, together with their almost null toxicity and total biodegradability, makes these solvents a suitable platform for developing gas separation agents within the green chemistry framework. Therefore, because of the promising characteristics of DESs as CO_2 absorbents and in general as gas separating agents, the state of the art on physicochemical properties of DESs in relationship to their influence on gas separation mechanisms and on the studies of gas solubility in DESs are discussed. The objective of this review work is to analyze the current knowledge on gas separation using DESs, comparing the capturing abilities and properties of DESs with those of ILs, inferring the weaknesses and strengths of DESs, and proposing future research directions on this subject.

1. INTRODUCTION

Worldwide carbon dioxide (CO_2) emissions have been continually increasing these last decades,[1] which has strong climate effects due to greenhouse gas effects.[2] CO_2 atmospheric levels reached the 400 ppm milestone in 2014 for the first time in human history, which, combined with the increasing yearly CO_2 emission rates,[1,3,4] shows the urgent need to limit and mitigate CO_2 emissions.[5,6] The increasing atmospheric CO_2 levels rise mainly from fossil fuel combustion for electricity production, transportation purposes, land use practices, and other human activities.[7] CO_2 emissions coming from energy-related operations have developed a pivotal role in comparison with other CO_2 sources,[8] and thus, controlling these emissions could lead to a remarkable decrease in CO_2 emission rates in a reasonable time frame. The first choice for mitigating CO_2 emission from energy-related operations would be moving from fossil fuels to renewable energy production methods.[9] Nevertheless, in spite of the increasing research on energy production from renewable sources,[10] which has led to an increasing role of these sources in the energy production pool,[11] fossil-fuel-based power plants are still the most viable solution for power and electricity generation because of major economic concerns.[12,13] Therefore, from a purely realistic viewpoint, developing CO_2 capturing technologies[14] would be the most feasible option for cutting CO_2 emissions in the next years without hindering technological and economic development.[15] In view of these facts, several multinational and multidisciplinary research programs are under development for obtaining suitable CO_2 capturing and gas separation technologies.[16]

A plethora of approaches for CO_2 capture from fossil-fueled power plants have been studied these last years.[17−22] CO_2 capture may be carried out using postcombustion, precombustion, and oxy-fuel approaches,[17,22] and although drawbacks and advantages may be considered for each approach,[17] post-combustion methods are employed more than precombustion applications for technical and economic reasons.[23−25] The technological problem of postcombustion CO_2 capture is basically a problem of gas separation from CO_2/N_2 mixtures, with the main difficulties rising from the low CO_2 partial pressure (roughly 0.15 atm). It should be remarked that CO_2 capture is a very energy-intensive process, and almost 80% of the total costs for the whole CO_2 mitigation effort are related to the capture process.[26] Therefore, developing suitable and effective sorbent materials for high-performance postcombustion CO_2 capturing purposes is the key step to allow sustainable uses of fossil fuels as a transition stage to a low-carbon economy and decrease the emissions of greenhouse gases through viable technologies at reasonable costs.

The most established postcombustion CO_2 capturing technologies employ aqueous amine solutions,[27,28] and they are still considered as the reference method in benchmarking of the other alternatives.[29] Nevertheless, amine-based technologies have serious drawbacks such as amine degradation,[30] high equipment corrosion,[31] large energy consumption for solvent regeneration,[32,33] and high operational costs.[34−37] Therefore,

Figure 1. Most common structures of hydrogen-bond donors and halide salts used in the preparation of DESs.

although developments in amine-based capturing methods have been proposed to solve the aforementioned problems,[38−42] the development of new materials for CO_2 capturing purposes with better properties than amine-based sorbents has attracted great attention in the literature elsewhere.[21,43−47] Ionic liquids (ILs) are a very promising alternative absorbent option for improving

the current status of postcombustion CO_2 capturing and gas separation technologies.[48−55] The wide interest in ILs arises from a general need for environmentally friendly new green solvents to replace common organic ones, which present several problems such as inherent toxicity or high volatility.[56−58] The remarkable interest in ILs developed both in industry and academia this past decade[59,60] arises from the physicochemical propertie of ILs,[61] which may be fine-tuned through suitable anion−cation combinations,[62−64] and from the possibility of developing task-specific ILs[65] for many applications,[66−71] including carbon capture purposes. Many of the physicochemical properties of ILs are very suitable for carbon capture purposes, such as almost negligible vapor pressure,[72] high thermal stability,[73,74] and low flammability,[75] which can be controlled through the selection of the involved ions. Nevertheless, in spite of all these possible benefits, the literature has also dealt with the problems and limitations of ILs. Indeed, many reports have pointed out the toxicity,[76] poor biodegradability,[77,78] combustible character,[79] unfavorable physical properties such as high viscosity,[80] or high-cost production of ILs.[81] Many of these drawbacks of ILs can be avoided through suitable selection or design considering the large amount of available ILs,[82] and thus, nontoxic,[83] highly biodegradable,[84] low-viscosity,[49,85] and cheap ILs[81] can be found in the literature.

In spite of the possibility of finding suitable candidates for many IL technological applications, including gas separation purposes, other approaches are being developed to take advantage of IL properties while avoiding their negative aspects. Deep eutectic solvents (DESs) are emerging as an alternative to ILs that provide similar features. DESs are a mixture of two or more components with a melting point lower than either of its individual components.[86,87] DESs are typically, but not always, obtained by mixing a quaternary ammonium halide salt, a hydrogen-bond acceptor (HBA), with a hydrogen-bond donor (HBD) molecule, which should be able to form a complex with the halide, leading to a significant depression of the freezing point.[88,89] For some compounds, a melting point is even not found, and a glass transition temperature is obtained; thus, DESs are also known as low-transition-temperature mixtures (LTTMs).[90] Nevertheless, the term DES will be used throughout this work to avoid any confusion. Though DESs are (mainly) constituted by ions, they are not ILs since they are not composed entirely of ions.

Since the first DES reported by Abbott et al.,[86] based on the salt choline chloride (CH_Cl) and urea in a 1:2 molar ratio, other combinations of HBDs and HBAs have been explored. Nevertheless, most of the DESs studied in the literature are CH_Cl-based in combination with very different types of HBDs. Other salts, such as imidazolium-,[91] ammonium-,[92,93] and phosphonium-based[94,95] ones, have also been studied, but to a minor extent in comparison with CH_Cl-based ones. Figure 1 summarizes the chemical structures along with their molar ratios for the most common DESs in the literature. The reasons for the large interest in CH_Cl-based DESs arises from the low cost, low toxicity,[96] biodegradability, and biocompatibility of the salt.[97] CH_Cl which is considered as an essential nutrient, can be extracted from biomass and often is regarded as a component of B-complex vitamins. Therefore, although new effects arise in DESs from the mixture formation in comparison with the properties of pure CH_Cl because of synergistic effects or from the HBA−HBD interactions,[98] CH_Cl-based DESs are a suitable platform for DES development considering

environmental, economic, and technological viewpoints. Further, DESs provide other interesting advantages in comparison with pure ILs, such as the fact that DES preparation may be carried out with 100% atom economy[99] without purification being required, which would favor large-scale applications of DESs. Likewise, advantages of DESs such as wide liquid range, water compatibility, low vapor pressure, nonflammability, biocompability, and biodegradability favor their use in many possible technologies.[87,89,100] DESs can be also obtained from natural sources (so-called natural DESs), particularly through primary metabolites such as organic acids, amino acids, and sugars.[101,102] The diversity of possible combinations of the starting materials provides a powerful tool to control the physical properties of DESs. Besides, DESs exhibit physiochemical properties similar to those of ILs, which, along with their advantages, allows DES to replace or improve upon ILs in many applications. In this sense, several review works have focused on the wide range of applications of DESs, such as organic synthesis, catalysis, biodiesel transformation, electrochemistry, nanotechnology, and separation technologies.[89,100]

Because of their many similarities with ILs, CO_2 capture using DESs has also been considered in the literature. Current research is devoted to experimental measurement of CO_2 solubility under different conditions such as pressure, temperature, and molar ratio of the two DES components as well as the effect of the HBD molecule.[58,87] Therefore, in this review we analyze the latest state of the art on CO_2 capture using DESs, considering general trends, key points, and the outlook for task-specific CO_2 capture using DESs. Moreover, reflecting the great interest that pure ILs have attracted for carbon capture purposes but also the serious drawbacks of some of the studied ILs, the feasibility of CO_2 capture with DESs in comparison with pure ILs will be discussed with the purpose of finding whether DES absorbents are suitable solutions for the problems and limitations of ILs from the technological and environmental viewpoints.[103] Since carbon capture from flue gases in postcombustion processes is a major technological problem, the available DES literature is also analyzed to assess whether DES-based separation processes such as general acid gas capture, with special attention to SO_2 absorption, and natural gas sweetening are viable.[48] Many of the doubts that have been raised concerning the development of economical and technologically feasible carbon capture and gas separation methods based on ILs at an industrial scale are based on the characteristics of IL physicochemical properties.[48,52,53] In particular, the large viscosity of many ILs would hinder heat and mainly mass transfer efficiency and increase pumping costs.[53,104] Despite the possibility of the design of low-viscosity ILs,[105−107] the question that rises is whether DES absorbents are a suitable alternative to avoid the aforementioned problems. Therefore, the available literature on the physicochemical properties of DESs is also studied because of the large number of possible DESs with very different physicochemical properties that can be considered and the importance of these properties for developing viable CO_2 capture[108] and gas separation processes using DESs.

2. PHYSICOCHEMICAL PROPERTIES

The interest in the application of DESs for gas separation technologies has led to the need for accurate and reliable knowledge of their physicochemical properties. This has led to further developments in process design and optimization for

gas separation purposes.[109,110] Therefore, the number of published works devoted to or reporting relevant physicochemical properties of DESs has increased in recent years. In Figure 2, the available literature on physicochemical properties of
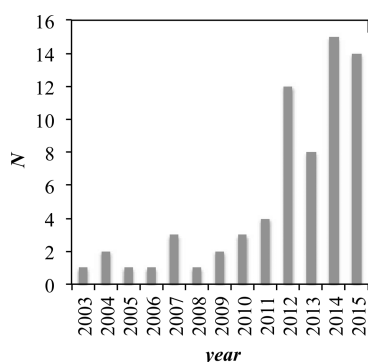

Figure 2. Number of publications (*N*) published in the 2003−2015 period containing experimental studies on the physical properties of DESs. Data for 2015 are through Feb 16, 2015.

DESs is summarized. The number of available studies in the period from 2003 (the year in which Abbott et al.[86] proposed for the first time the use of a DES) to 2011 is very small, whereas the interest in the physicochemical properties of DESs has increased remarkably starting from 2012, as evidenced by the number of general DES publications in the same period.[58] Nevertheless, the physicochemical studies available in the literature are still very scarce considering the size and importance of the research field (Figure 2). Therefore, the available literature on physicochemical information for DESs will be analyzed in the next section(s) to infer the weaknesses and strengths of the current state of the art and the future needs. The most relevant physicochemical properties are selected by considering their relevance for DES characterization and CO_2/gas separation purposes.

Melting Temperature and Solid−Liquid Phase Equilibria. DESs are formed by the mixing of HBAs (ILs) and HBDs in suitable amounts. Most of the available literature considers only binary DESs (i.e., mixtures of one type of HBA and one type of HBD), although ternary DESs have also been reported in the literature.[111] The main characteristics of the solid−liquid phase diagrams for these binary DESs are summarized in Figure 3. It should be noted that the eutectic composition is a single value that corresponds to the minimum melting temperature in the phase diagram, as reported in Figure 3. The very low melting points of DESs in comparison with those for the salts (HBAs) and HBDs forming them is one of their most relevant and distinct known properties. For instance, in the case of CH_Cl + urea, which form a DES at a 1:2 salt:urea molar ratio, the melting point of DES is 285.15 K,[86] whereas those for pure CH_Cl and urea are 575.15 and 407.15 K, respectively. This melting point depression upon mixing arises from the development of strong HBA−HBD intermolecular interactions, which are optimal for the eutectic mixture composition.

The temperatures for the melting points of selected DESs are summarized in Table 1, although DESs with melting points as high as 473 K may be found in the literature,[87] only those with melting points close to the ambient temperature are attractive for practical purposes such as minimizing the energy penalty for melting those high temperature DESs. Therefore, only DESs
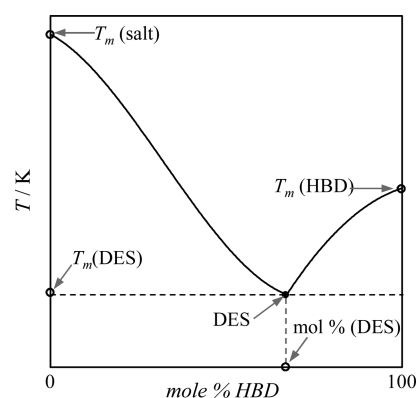

Figure 3. Schematic solid−liquid phase diagram for a binary mixture between a salt and an HBD, showing the appearance of the DES at the mixture composition and temperature marked in the figure. T_m stands for the melting point. The solid line shows the melting point temperature as a function of mixture composition, and the dashed lines show the temperature and composition of the eutectic mixture.

with melting points lower than 333.15 K are included in Table 1. Analysis of the data reported in Table 1 shows that most of the available studies consider CH_Cl-based DESs involving HBDs belonging to three main types of compounds: nitrogen-based compounds, alcohols, and carboxylic acids. Additional relevant studies are centered in phosphonium- and alkylammonium-based cations. The lower melting points for the considered CH_Cl-based DESs reported in Table 1 are obtained for those DESs involving polyols, such as glycerol or ethylene glycol. Likewise, a very low melting point is obtained for 2,2,2-trifluoroacetamide, which confirms the role of the hydrogen-bonding ability of the HBD in lowering the melting point.[87]

Nevertheless, in spite of the strong effect of HBD properties on the CH_Cl-based DES melting point, structure−property relationships are not available in the literature. Therefore, in view of the large number of possible HBDs for developing DESs and the need to develop low-melting DESs for practical purposes, a quantitative structure−activity relationship (QSAR) predictive model was developed in this work for CH_Cl-based DESs. This model was limited to CH_Cl-based DESs because the available literature information for other types of DESs is scarce, and thus, QSAR models could not be developed for other salts because of statistical restrictions. In order to carry out QSAR modeling, 29 HBDs developing DESs with CH_Cl in 1:0.5, 1:1, 1:2, or 1:4 molar ratios were selected from the literature (Table S1 in the Supporting Information). The molecular structures of the selected HBDs were optimized at the B3LYP/6-31+G* theoretical level using the Gaussian 09 simulation software package.[128] To develop the QSAR model, 335 molecular descriptors were calculated for each HBD using the QSAR module of Materials Studio software[129] (Table S2 in the Supporting Information). Significant descriptors were selected by considering the genetic function approximation using the same simulation software and were used for the development of the prediction model using literature melting point data (Table 1) for the 29 selected HBDs as training set with the genetic algorithm approach in Materials Studio. A seven-parameter model was selected, and although slight modifications in the correlative and predictive ability of the model could be obtained increasing the number of model parameters, this was not considered in order to avoid

Table 1. Melting Temperatures (T_m) of Selected DESs (Only Low-Melting DESs, with $T_m < 333.15$ K, Are Reported for Practical Purposes)

salt	HBD	salt:HBD molar ratio	T_m/K	ref
choline chloride	urea	1:2	285.15	86
choline fluoride	urea	1:2	274.15	86
choline nitrate	urea	1:2	277.15	86
choline chloride	1-methylurea	1:2	302.15	86
choline chloride	acetamide	1:2	324.15	86
choline chloride	2,2,2-trifluoroacetamide	1:2.5	228.15	112
choline chloride	glycerol	1:2	233.15	113
choline chloride	ethylene glycol	1:2	207.15	112
choline chloride	1,4-butanediol	1:3	241.15	83
choline chloride	imidazole	3:7	329.15	91
choline chloride	malonic acid	1:1	283.15	114
choline chloride	oxalic acid	1:1	307.15	114
choline chloride	lactic acid	1:2	195.42[a]	116
choline chloride	malic acid	1:1	216.67[a]	116
choline chloride	oxalic acid dihydrate	1:1	232.98[a]	116
choline chloride	phenylacetic acid	1:2	298.15	114
choline chloride	phenylpropionic acid	1:2	293.15	114
choline chloride	glutaric acid	1:1	256.37[a]	118
choline chloride	glycolic acid	1:1	257.08[a]	118
choline chloride	levulinic acid	1:2	–[b]	119
choline chloride	itaconic acid	1:1	330.15	119
choline chloride	L-(+)-tartaric acid	1:0.5	320.15	119
choline chloride	xylitol	1:1	–[b]	119
choline chloride	D-sorbitol	1:1	–[b]	119
choline chloride	D-isosorbide	1:2	–[b]	119
choline chloride	D-fructose	2:1	283.15	120
choline chloride	D-glucose	2:1	288.15	122
choline chloride	phenol	1:3	253.1	123
choline chloride	o-cresol	1:3	249.4	123
choline chloride	xylenol	1:3	290.8	123
choline chloride	ZnBr₂	1:2	311.15	124
choline chloride	SnCl₂	1:2	310.15	124
choline acetate	glycerol	1:1.5	286.15	126
choline acetate	urea	1:2	291.15	126
choline acetate	ethylene glycol	1:2	296.15	126
2-acetyloxy-N,N,N-trimethylethanaminium chloride	ZnBr₂	1:2	321.15	124
2-acetyloxy-N,N,N-trimethylethanaminium chloride	SnCl₂	1:2	293.15	124
N-(2-hydroxyethyl)-N,N-dimethylanilinium chloride	SnCl₂	1:2	290.15	124
N-(2-hydroxyethyl)-N,N-dimethylanilinium chloride	FeCl₃	1:2	294.15	124
N-ethyl-2-hydroxy-N,N-dimethylethanaminium chloride	urea	1:2	235.15	86
N-benzyl-2-hydroxy-N,N-dimethylethanaminium cloride	urea	1:2	240.15	86
N,N,N-trimethyl(phenyl)methanaminium chloride	urea	1:2	299.15	86
2-(acetyloxy)-N,N,N-trimethylethanaminium chloride	urea	1:2	259.15	86
2-chloro-N,N,N-trimethylethanaminium chloride	urea	1:2	288.15	86
N-benzyl-2-hydroxy-N-(2-hydroxyethyl)-N-methylethanaminium chloride	urea	1:2	267.15	86
2-fluoro-N,N,N-trimethylethanaminium bromide	urea	1:2	328.15	86
ethylammonium chloride	urea	1:1.5	302.15	115
ethylammonium chloride	methylurea	1:1.5	302.15	115
ethylammonium chloride	1-(trifluoromethyl)urea	1:1.5	293.15	115
tetrabutylammonium bromide	imidazole	3:7	294.15	91
1-ethyl-3-butylbenzotriazolium hexafluorophosphate	imidazole	1:4	330.15	91
tetrabutylammonium chloride	glycerol	1:5	230.37	117
tetrabutylammonium chloride	ethylene glycol	1:3	242.27	117
tetrabutylammonium chloride	triethylene glycol	3:1	260.46	117
methyltriphenylphosphonium bromide	glycerol	1:3	267.60	83, 92
methyltriphenylphosphonium bromide	ethylene glycol	1:4	223.80	83, 92
methyltriphenylphosphonium bromide	triethylene glycol	1:5.25	251.60	83
N,N-diethylethanolammonium chloride	glycerol	1:2	271.82	92
N,N-diethylethanolammonium chloride	ethylene glycol	1:2	242.15	92
N,N-diethylethanolammonium chloride	triethylene glycol	1:2	273.05	83
methyltriphenylphosphonium bromide	glycerol	1:3	267.6	121
methyltriphenylphosphonium bromide	ethylene glycol	1:4	223.8	121
methyltriphenylphosphonium bromide	triethylene glycol	1:5	251.6	121
methyltriphenylphosphonium bromide	2,2,2-trifluoroacetamide	1:8	203.86	94
benzyltriphenylphosphonium chloride	glycerol	1:5	323.51	94
benzyltriphenylphosphonium chloride	ethylene glycol	1.3	321.06	94
tetrapropylammonium bromide	glycol	1:3	257.05	125
tetrapropylammonium bromide	ethylene glycol	1:4	249.75	125
tetrapropylammonium bromide	triethylene glycol	1:3	253.95	125
lithium bis[(trifluoromethyl)sulfonyl]imide	N-methylacetamide	1:4	201.05[a]	127
1-butyl-3-methylimidazolium chloride	ZnCl₂	1:1	223.05	111

[a] Glass transition temperature. [b] Liquid at room temperature but T_m not available.

overfitting. Statistical parameters of the QSAR model are reported in Table S3 in the Supporting Information. The proposed QSAR model leads not only to excellent correlative ability ($R^2 = 0.97$; Figure 4) but also to high predictive ability,
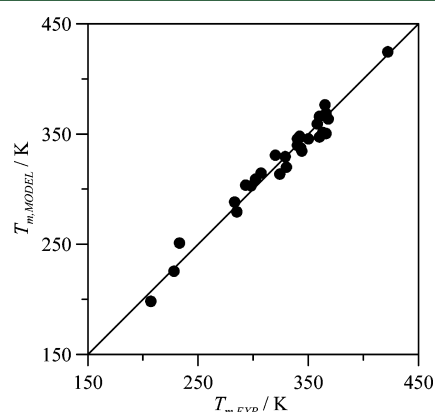

Figure 4. Comparison of melting points of CH_Cl-based DESs predicted using the QSAR model ($T_{m,MODEL}$) with the experimental values ($T_{m,EXP}$). The selected DESs for training of the QSAR model are reported in Table S1 in the Supporting Information, and the statistical parameters of the model are shown in Table S3 in the Supporting Information. A line showing the perfect correlation is included in the figure for comparison purposes.

as shown by the obtained cross-validated R^2 value of 0.93. Therefore, it is possible to develop accurate predictive structure−property relationships for melting points of DESs. Nevertheless, further experimental measurements studying additional HBDs and other types of ILs are required in order to extend the proposed QSAR approach in a systematic way. These additional experimental needs should be remarked considering the information summarized in Table 1, which points to the remarkable role on the DES melting point played not only by the HBD but also by the involved IL (salt).

Vapor Pressure and DES Volatility. One of the most remarkable physical properties of ILs is their almost null vapor pressure.[130,131] Therefore, ILs could replace volatile organic compounds, avoiding any atmospheric pollution and also the corresponding hazards for worker exposure or derived risks such as vapor flammability on their industrial use.[132] As DESs are formed by mixing a nonvolatile compound, the IL, plus a volatile compound, they should have larger volatilities than pure ILs, and thus, the question that arises is whether DESs have low enough volatility to maintain the advantages of ILs. The available literature on experimental measurements of DES vapor pressure is extremely scarce. Boisset et al.[127] showed that the DES formed from lithium bis[(trifluoromethyl)sulfonyl]-imide and N-methylacetamide in a 1:4 molar ratio has a vapor pressure of 0.2 mbar at 313.15 K, which is several orders of magnitude lower than for the most common organic solvents. Nevertheless, in the case of this bis[(trifluoromethyl)sulfonyl]-imide + N-methylacetamide DES, it should be remarked that both compounds of the mixture have very low vapor pressures (0.5 mbar at 313.15 K has been reported for pure N-methylacetamide[133]), and thus, the change in vapor pressure upon mixing is not very remarkable. Analysis of the available literature has not led to any other vapor pressure studies for pure DESs, but Wu et al.[134] reported vapor pressure measurements for CH_Cl + urea, + ethylene glycol, + glycerol, or + malonic acid in water mixtures in the 303.15−343.15 K

temperature range for DES concentrations up to 80 wt %. These results showed a remarkable decrease in vapor pressure in comparison with pure water as the DES concentration increased, and in the case of 80 wt % DES concentration, the vapor pressures were in the 16−20 mbar range at 303.15 K for the four studied DESs. Thus, although these mixtures do not correspond to pure DESs and lower vapor pressure values should therefore be obtained for 100 wt % DES systems, the vapor pressures of these CH_Cl systems studied by Wu et al.[134] should be larger than those for the bis[(trifluoromethyl)-sulfonyl]imide + N-methylacetamide DES studied by Boissett et al.,[127] thereby showing the role played by the HBD on the DES volatility. Wu et al.[134] also showed that the lower the melting point, the lower is the vapor pressure, although this effect should be very weak considering that the CH_Cl-based DESs studied by Wu et al.[134] have melting points in the 207.15−285.15 K range whereas the vapor pressures for 80 wt % aqueous solutions show differences of only 4 mbar. Nevertheless, although pure CH_Cl-based DESs were not studied by Wu et al.,[134] from their reported results for aqueous solutions it may be inferred that these are low-volatility compounds in comparison with common organic solvents. Likewise, the scarcity of the literature on DES vapor−liquid equilibria shows the need for systematic studies of this property as a function of salt and HBD types at different temperatures.

Density. The relevance of density for process design purposes is well-known.[110] Likewise, the temperature and pressure effects on density (PVT behavior) is required for the development of suitable equations of state, which play a pivotal role in the calculation of thermodynamic properties required for the development of industrial processes,[135] including gas separation operations. Density is a thermophysical property that has been more studied for DESs, and most of the considered DES have densities in the 1.0−1.35 g cm^{-3} range at 298.15 K, although those DES containing metallic salts such as ZnCl$_2$ have densities in the 1.3−1.6 g cm^{-3} range.[87]

In a previous work,[61] it was reported the remarkable differences between the densities of ILs obtained from different literature sources arise from the used experimental methods and sample qualities. Therefore, it was necessary to analyze whether any disagreement between the DES density values was obtained, in spite of the fact that the number of available studies for DESs is remarkably lower than that for pure ILs. First, the literature for the CH_Cl + urea (1:2 molar ratio) DES (summarized in Table 2) show that differences of up to 4% between the available literature sources may be inferred. These

Table 2. Densities (ρ) of the CH_Cl + Urea (1:2 Molar Ratio) DES from Different Literature Sources^a

T/K	$\rho/\text{g cm}^{-3}$	sample origin	method	ref
313.15	1.24	prepared	not stated	115
298.15	1.25	commercial	not stated	136
298.15	1.212	prepared	vibrating tube	137
298.15	1.1979	commercial	vibrating tube	138
313.15	1.1893	commercial	vibrating tube	138
313.15	1.1887	commercial	vibrating tube	139
298.15	1.20	prepared	tensiometer	140

^{a}The sample origin column shows whether the DES was prepared for the corresponding study by mixing the two components or purchased from a commercial supplier. The experimental method used is also reported. All values were measured at 0.1 MPa.

differences are significant and may have important effects on process design,[110] and they may be justified considering the different applied experimental methods and (more importantly in our opinion) the quality, method of preparation, and impurities of the samples used. This is confirmed by an analysis of density data for CH_Cl + glycerol (Figure 5), which shows
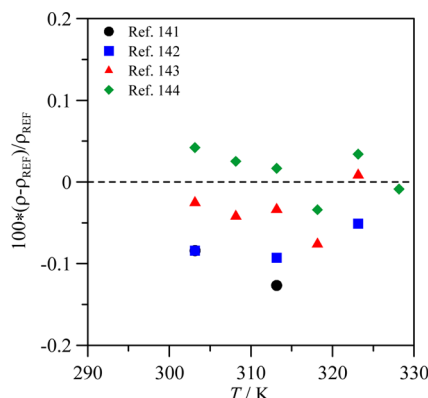

Figure 5. Comparison of literature density data for the CH_Cl + glycerol (1:2 molar ratio) DES.[141−144] Reference density data (ρ_{REF}) for comparison purposes were obtained from Shahbaz et al.[92] All values were measured at 0.1 MPa.

excellent agreement among all of the literatures sources. The main difference between the results in Table 2 and Figure 5 is that samples used for the measurements reported in Figure 5 were properly characterized, including impurities and water contents, which have a strong effect on density, whereas this is not true for all of the data reported in Table 2. Moreover, Florindo et al.[118] reported that the method of DES preparation (heating of the mixture or grinding) also has an effect on the DES thermophysical properties, and although this effect is larger for viscosity than for density, it should also be considered for comparison purposes. Therefore, problems analogous to those reported for pure ILs appear for DESs, and thus, properly defined measurements should be carried out by paying special attention to the characterization of the samples used.

The effect of the HBD molecular type on the DES density is analyzed in Figure 6 for CH_Cl-based DES systems. The molecular characteristics of the HBD and the molar ratio at which the DES is formed have a large effect on the density of

the DES and its temperature variation (isobaric thermal expansion coefficient, α_p). The data reported in Figure 6a show very large densities for 1:3 DES formed by ethanolamine or 2,2,2-trifluoroacetamide, but for these DES the temperature effect on density is remarkably larger than for the remaining DES leading to α_p values roughly three times larger. In the case of DES formed by HBD with hydroxyl groups, density increases with the number of hydroxyl groups (larger values for glycerol than for ethylene glycol) and decreases with the introduction of aromatic groups (lower values for phenol, which is the DES with lower densities among all the studied ones in Figure 6). In the case of diacid DES, density decreases with increasing chain length (oxalic > malonic > glutaric). Therefore, steric effects (the salt:HBD molar ratio) and the strength and extension of ions − HBD determines the behavior of density for the analyzed DES.

The volumetric effects of the mixing of the salt and the corresponding HBD may be analyzed by considering the so-called free volume (V_{free}). This may be calculated as the difference between the hard-core volumes obtained from the calculated molecular volumes of the involved compounds and the corresponding molar volume calculated from the experimental density, according the procedure reported by Abbott et al.[113] Hard-core volumes were obtained from the optimized structures of the CH_Cl ion pair and the corresponding HBD, calculated at B3LYP/6-31+G* theoretical level,[128] according to the Connolly method. The percentage contributions of the free volume to the total molar volume (% V_{free}) for CH_Cl + HBD DESs are reported in Figure 7. The results show that DESs with 1:1 and 1:2 molar ratios lead to % V_{free} = 25−28% with a weak effect of the type of HBD. For the 1:3 CH_Cl-based DES with phenol as the HBD, %V_{free} is slightly larger than for the 1:1 and 1:2 DESs, but in the case of ethanolamine and 2,2,2-trifluoroacetamide as the HBD, the behavior is completely different, leading to very low or very high %V_{free}. This behavior is in agreement with the behaviors of the density and thermal expansion coefficient reported in Figure 6.

The type of salt involved in DES has also a strong effect on the DES volumetric properties, as shown in Figure 8. The reported results show that for a fixed HBD (ethylene glycol), ammonium-based DESs have lower densities that phosphonium-based DESs. In the case of the tetralkylammonium bromide DESs, increasing the length of the cation alkyl chain
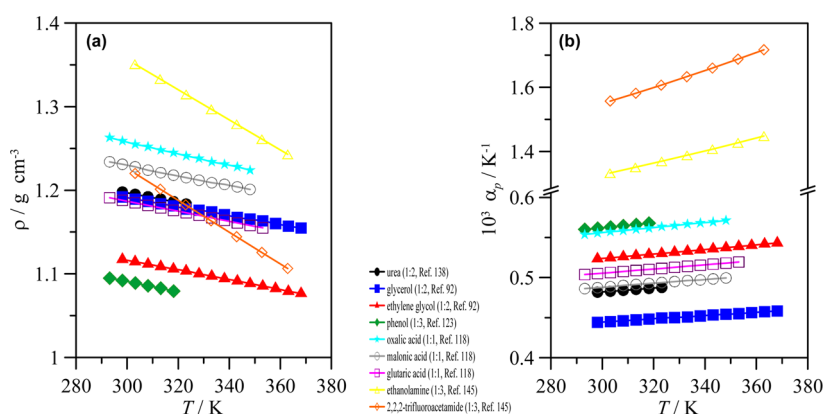

Figure 6. Effect of the HBD on (a) the density (ρ) and (b) the isobaric thermal expansion coefficient (α_p) for CH_Cl + HBD DESs.[92,118,123,138,145] All values were measured at 0.1 MPa. The α_p values in (b) were calculated from the linear fits (solid lines) reported in (a). The oxalic, malonic, and glutaric acid data reported in ref 118 were for dried samples. The molar ratio of each DES is indicated in the figure labeling.
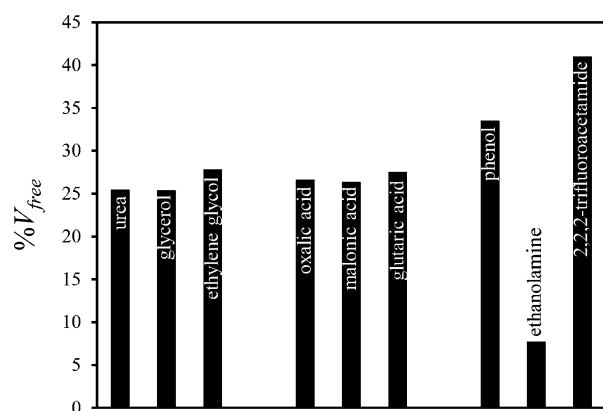
Figure 7. Values $\%V_{free}$ calculated according to the procedure of Abbott et al.[113] for CH_Cl + HBD DESs. All values were determined at 303.15 K. Values for urea, glycerol, and ethylene glycol correspond to 1:2 DESs, those for oxalic, malonic, and glutaric acid to 1:1 DESs, and those for phenol, ethanolamine, and 2,2,2-trifluoroacetamide to 1:3 DESs. Density values used for the $\%V_{free}$ calculations were obtained from refs 92, 123, 138, and 145.

decreases the density (e.g., by 5% at 303.15 K in going from propyl to butyl chains; Figure 8a). Likewise, the anion type also has an effect on the DES density, even when only halogen anions are considered, as bromide salts lead to denser DESs than chloride ones (e.g., the tetrabutylmmonium bromide DES is 3.6% denser than the tetrabutylammonium chloride DES at 303.15 K; Figure 8a). The effect of the salt type on the behavior of the isobaric thermal expansion coefficient is reported in Figure 8b. Increasing the alkyl-chain length in alkylammonium-based DESs increases the compressibility, which may be justified by considering the increasing free volume. Bromide-containing DESs are also more compressible than chloride ones, which may be justified by considering both the larger free volumes for DESs containing bulkier anions and the weaker anion−cation and anion−HBD interactions for larger anions. It should be remarked that phosphonium-based DESs, in spite of being denser than alkylammonium ones, have compressibilities in the same range as the alkylammonium and cholinium DESs.

Most of the available literature on the volumetric properties of DESs reports results only under atmospheric pressure conditions, and studies of the PVT behavior of DESs are very

scarce. To our knowledge, PVT studies of DESs have been reported only for CH_Cl-based systems with urea,[138] glycerol,[143] or ethylene glycol,[147] and all of them were reported by the same research group (Li et al.). This source exhibits only an analysis of the effect of the HBD on the DES PVT properties (Figure 9). Isothermal compressibility (κ_T) data are available
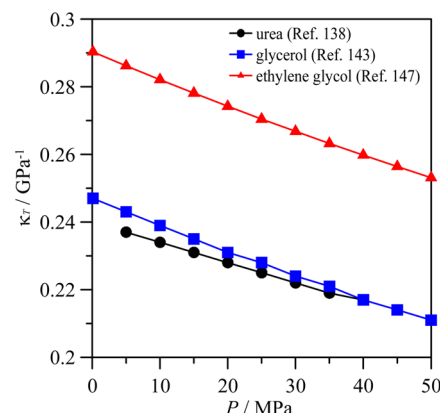

Figure 9. Isothermal compressibility (κ_T) for CH_Cl + HBD 1:2 DESs at 313.15 K.

for CH_Cl-based DESs, showing that using ethylene glycol as the HBD leads to the most compressible DES in comparison with those based on urea and glycol. The rates of decrease of κ_T with increasing pressure are −0.00058, −0.00072, and −0.00075 GPa^{-1} K^{-1} for urea, glycol, and ethylene glycol, respectively, showing moderate effects of pressure on the volumetric properties for the three studied DESs up to 50 MPa. This behavior points to strong intermolecular interactions between the IL and the corresponding HBDs that are only weakly affected by the pressure (Figure 9). The available PVT results for CH_Cl-based DESs allow the calculation of the internal pressure ($P_i = T\alpha_p/\kappa_T − P$). P_i is thermodynamically defined as the change in the fluid's internal energy per mole upon small isothermal expansion. Therefore, P_i may be used to quantify the strength of the intermolecular forces in fluids,[57] although it is well-known that the cohesive energy (c), which may be inferred from the vaporization enthalpy, measures the total strength of the intermolecular forces and that $c > P_i$ because P_i quantifies mainly weak intermolecular forces,[148]
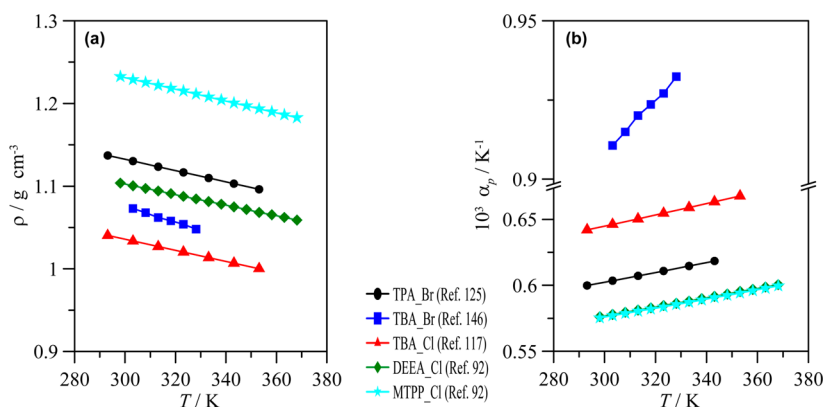

Figure 8. Effect of the IL on (a) the density (ρ) and (b) the isobaric thermal expansion coefficient (α_p) for IL + ethylene glycol DESs. All values were obtained at 0.1 MPa. The α_p values in (b) were calculated from the linear fits (solid lines) reported in (a). A 1:4 molar ratio was used for all of the reported DESs. Acronyms: TPA_Br, tetrapropylammonium bromide;[125] TBA_Br, tetrabutylammonium bromide;[146] TBA_Cl, tetrabutylammonium chloride;[117] DEEA_Cl, N,N-diethanolammonium chloride;[92] MTPP_Br, methyltriphenylphosphonium bromide.[92]

which are preferentially affected by small expansions. Therefore, the internal pressures for CH_Cl-based DESs were calculated from literature PVT data and are reported in Table 3. The P_i

Table 3. Internal Pressure (P_i) for CH_Cl + HBD 1:2 DESs at 303.15 K Calculated from PVT Data Reported in the Literature[138,143,147]

HBD	P_i/MPa	
	P = 5 MPa	P = 45 MPa
urea	612.5	617.6
glycerol	607.2	624.7
ethylene glycol	542.2	538.2

values for the reported CH_Cl-based DESs are large, even larger than those for many viscous ILs,[149,150] which shows that the main characteristics of DESs arise from the strong intermolecular forces developed between the salt and the HBD. The results in Table 3 show that ethylene glycol leads to lower P_i than urea and glycerol, which show equivalent values; this would justify the larger compressibilities reported in Figures 6 and 9.

The large number of possible salt−HBD combinations, together with the practical importance of density for industrial applications, leads to the need for the development of predictive models and structure−property relationships that allow effective screening of DESs. Nevertheless, only the research group led by Mjalli[92,144,151] has carried out a systematic research effort to test the predictive ability of several theoretical approaches for the prediction of density in ammonium- and phosphonium-based DESs. In a first approach, density modeling was carried out by a thermodynamic approach using the Rackett and Guggenheim methods combined with the modified Lydersen−Joback−Reid group contribution or Eötvos methods for the prediction of critical properties.[144,151] It should be remarked that the predictive

ability of these methods stands on the availability of critical properties, which in the absence of experimental information for DESs are predicted using two different methods. The analysis of critical temperatures reported by Mjalli and co-workers[144] showed very different values for the two methods (e.g., for the CH_Cl + glycerol 1:2 DES, values of 680.7 and 1075.3 K were obtained using the Joback and Eötvos methods, respectively), which discards any physical interpretation of these properties. The predictive ability of these two approaches is reasonable, leading to deviations of less than 2% with respect to the experimental results, but they give poor predictions of the temperature dependence of the density, thus limiting their applicability only to temperatures close to ambient conditions. An alternative model development was carried out using the neural network approach,[92] leading to very satisfactory predictions with average deviations of 0.14% with respect to the experimental results and good predictive abilities at high temperatures, in contrast to previous thermodynamic methods. Nevertheless, the suitability of this neural-network-based approach has to be analyzed against a larger database of DESs, as in the work by Shahbaz et al.[92] only two HBDs (glycerol and ethylene glycol) and three salts (CH_Cl, N,N-diethylethanolammonium chloride, and methyltriphenylphosphonium bromide) were considered. Although the temperature and DES composition effects were analyzed, the effect of the molecular structures of the salt and HBD on the model predictability should be considered.

Viscosity. This property has been extensively measured for the available DESs because of its importance for industrial purposes. Nevertheless, all of the studies were carried out at atmospheric pressure, and thus, pressure−temperature−viscosity studies are required for future applications of DESs in fields such as lubrication[140] or any other potential high-pressure operation. Many DESs are highly viscous liquids,[87] e.g. the classic CH_Cl + urea (1:2 molar ratio) DES has a viscosity of 750 mPa s at 298.15 K. This is even worse for other families of

Table 4. Low-Viscosity DESs Available in the Open Literature (DESs with Viscosities Lower Than 500 mPa s Were Selected)

salt	HBD	salt:HBD molar ratio	T/K	η/mPa s	ref
choline chloride	urea	1:2	303.15	449	136
choline chloride	glycerol	1:2	303.15	246.79	142
choline chloride	ethylene glycol	1:2	303.15	35	136
choline chloride	glycolic acid	1:1	303.15	394.8	118
choline chloride	levulinic acid	1:2	303.15	164.5	118
choline chloride	phenol	1:3	303.15	35.17	123
choline chloride	o-cresol	1:3	298.15	77.65	123
N,N-diethylammonium chloride	glycerol	1:2	303.15	351.46	152
N,N-diethylammonium chloride	ethylene glycol	1:2	303.15	40.68	152
tetrapropylammonium bromide	ethylene glycol	1:3	303.15	58.2	125
tetrapropylammonium bromide	triethylene glycol	1:3	303.15	71.9	125
tetrabutylammonium bromide	imidazole	3:7	303.15	314.5	91[a]
tetrabutylammonium chloride	glycerol	1:4	303.15	476.1	117
tetrabutyl ammomium chloride	ethylene glycol	1:4	303.15	56.90	117
tetrabutylammonium bromide	glycerol	1:3	303.15	467.2	146
tetrabutylammonium bromide	ethylene glycol	1:3	303.15	77	146
tetrabutylammonium bromide	1,3-propanediol	1:3	303.15	135	146
tetrabutylammonium bromide	1,5-propanediol	1:3	303.15	183	146
methyltriphenylphosphonium bromide	ethylene glycol	1:4	298.15	109.8	94
methyltriphenylphosphonium bromide	2,2,2-trifluoroacetamide	1:8	298.15	136.15	94
lithium bis[(trifluoromethyl)sulfonyl]imide	N-methylacetamide	1:4	303.15	39	127

[a]Non-Newtonian fluid.

Table 5. Comparison of literature sources for DES viscosity, η. The sample origin column shows if the DES were prepared for the corresponding study mixing both components or the DES was purchased from a commercial supplier

salt	HBD	salt:HBD molar ratio	T/K	η/mPa s	sample origin[a]	method	ref
choline chloride	urea	1:2	303.15	152	prepared	rotational	86
			303.15	449	commercial	not reported	136
			303.15	527.28	commercial	rolling ball	139
choline chloride	glycerol	1:2	303.15	190	prepared	rotational	113
			303.15	188	commercial	not reported	136
			303.15	246.79	commercial	rolling ball	142
choline chloride	ethylene glycol	1:2	298.15	37	commercial	not reported	136
			298.15	41	prepared	rotational	137
choline chloride	malonic acid	1:1	303.15	982.9	prepared	Stabinger	118
			303.15	629	commercial	not reported	136
			303.15	464	prepared	rotational	114
			303.15	608	prepared	rotational	145
choline chloride	oxalic acid	1:1	313.15	1881	prepared	rotational	114
			313.15	2142	prepared	Stabinger	118
			313.15	202	prepared	rotational	145

[a]The sample origin column shows whether the DES was prepared for the corresponding study by mixing the two components or purchased from a commercial supplier.

DESs. For example, those based on sugar HBDs, which were recently proposed because of their good environmental properties, have extremely large viscosities (e.g., 34400 mPa s for CH_Cl + glucose in a 1:1 molar ratio at 323.15 K),[119] as do those containing metallic compounds, such as CH_Cl + ZnCl$_2$ in a 1:2 molar ratio (85000 mPa s at 298.15 K).[124] These large viscosities hinder many industrial applications and in particular give rise to important process design problems for CO$_2$ and gas separation purposes because of prohibitive pumping costs and poor heat and mass transfer, which would require equipment oversizing and thus lead to larger costs for CO$_2$ capturing operations. However, the low-viscosity DESs ($\eta < 500$ mPa s) available in the literature, which are reported in Table 4, show that it is possible to develop DESs with viscosities close to those of common organic solvents. The low viscosities of DESs containing ethylene glycol, phenol, or levulinic acid are especially remarkable for practical purposes.

Viscosity data for some of the most studied DESs are compared in Table 5 for the available literature sources. The analysis of the literature shows very large differences among the different sources for the same DES. These extremely large disagreements may rise from (*i*) experimental method, (*ii*) sample preparation procedures, and (*iii*) impurities. The method of preparation has an effect on the physical properties of DESs. Florindo et al.[118] reported differences of 6.5% between the viscosity data for DES samples prepared by the traditional heating and stirring method in comparison with a grinding approach. Nevertheless, the data reported in Table 5 were obtained for samples prepared according to the heating method, and the differences are remarkably larger than those that could be inferred from different preparation methods. The experimental method used to measure the viscosity could have an effect on the obtained viscosity data, and within this effect it should be remarked that Hou et al.[91] showed that some DESs are non-Newtonian fluids, which should be considered when analyzing their rheological properties. Nevertheless, in our opinion the most remarkable feature that could explain the scatter in the literature data is the presence of nonquantified impurities. Many types of DES are highly hygroscopic. For example, Yadav and Pandey[139] showed that the viscosity of CH_Cl + urea (1:2 molar ratio) at 303.15 K decreases from

527.3 to 200.6 mPa s in going from the pure DES to 0.1 water mole fraction. For very viscous DES systems, Florindo et al.[118] showed that CH_Cl + oxalic acid (1:1 molar ratio) can capture water from atmospheric moisture up to 19.40% water content, which decreases the viscosity at 303.15 K from 5363 to 44.49 mPa s. Therefore, the characterization of impurities, paying particular attention to the water content, is crucial for reporting accurate, reproducible, and reliable viscosity data. The problem of scatter in the literature viscosity data reported for ILs seems to extend to the DES literature,[61] and thus, systematic studies of the viscosity of DESs as a function of pressure, temperature, and composition are recommended.

The possibility of decreasing the viscosity of DESs by adding controlled amounts of water is a very attractive option for highly viscous DESs. Nevertheless, this should be done with caution since it may effect and change other properties of the DES remarkably. In the case of DESs for CO$_2$ capturing purposes, absorbed water may compete with CO$_2$ molecules for the absorption sites,[153] leading to a decrease in the CO$_2$ capturing ability of the DES.[154] Therefore, for very viscous fluids, a compromise solution between low viscosity and CO$_2$ affinity should be found.

The temperature has a large effect on DES viscosity, and thus, highly viscous DESs, which cannot be used for practical purposes at close to ambient conditions, could be considered for technical applications at higher temperatures. For example, the viscosity changes in going from 298 to 328 K for CH_Cl-containing DESs are 750 to 95 mPa s (for urea, 1:2 molar ratio), 259 to 52 mPa s (for glycerol, 1:2 molar ratio), and 1124 to 161 mPa s (for malonic acid, 1:1 molar ratio).[136] Even highly viscous sugar-based DESs show very large viscosity decreases with increasing temperature. For example, the viscosity of CH_Cl + glucose (2:1 molar ratio) changes from 7992 mPa s at 298.15 K to 262 mPa s at 328.15 K. The viscosity–temperature behavior of DESs is described satisfactorily in the literature following either Arrhenius[94,114,117,118,120,122,125,145] or Vogel–Fulcher–Tamman (VFT)[123,127,139,142,152] behavior. Fitting viscosity–temperature data to Arrhenius behavior allows calculation of the activation energy (E_a), which can be used to quantify the temperature dependence of the viscosity and the strength of the intermolecular forces in the DES and their

Table 6. Activation Energies (E_a) Calculated from Fits of Experimental Viscosity−Temperature Data to an Arrhenius-Type Model over the Indicated T Ranges

salt	HBD	salt:HBD molar ratio	T range/K	E_a/kJ mol^{-1}	ref
choline chloride	urea	1:2	298−328	−55.7	136[a]
choline chloride	glycerol	1:2	293.15−328.15	−45.1	113
choline chloride	ethylene glycol	1:2	298−328	−11.26	136[a]
choline chloride	oxalic acid	1:1	293.15−348.15	−65.20	118
choline chloride	malonic acid	1:1	293.15−348.15	−46.66	118
choline chloride	glutaric acid	1:1	293.15−353.15	−47.62	118
choline chloride	succinic acid	1:1	313.15−343.15	−74.1	114
choline chloride	citric acid	1:1	338.15−353.15	−66.7	114
choline chloride	phenylacetic acid	1:2	298.15−328.15	−52.5	114
choline chloride	phenylpropionic acid	1:2	308.15−318.15	−51.6	114
choline chloride	2,2,2-trifluoroacetamide	1:2	298.15−363.15	−32.40	145
choline chloride	D-glucose	2:1	298.15−358.15	−92.64	122
choline chloride	D-fructose	2:1	298.15−358.15	−57.70	120
tetrapropylammonium bromide	glycerol	1:3	293.15−353.15	−34.12	125
tetrapropylammonium bromide	ethylene glycol	1:3	293.15−353.15	−53.27	125
tetrabutylammonium chloride	glycerol	1:3	293.15−353.15	−52.21	117
tetrabutylammonium chloride	ethylene glycol	1:3	293.15−353.15	−32.72	117
methyltriphenylphosphonium bromide	glycerol	1:1.75	278.15−368.15	−64.46	94
methyltriphenylphosphonium bromide	ethylene glycol	1:4	278.15−368.15	−40.58	94
methyltriphenylphosphonium bromie	2,2,2-trifluoroacetamide	1:8	278.15−368.15	−46.68	94

[a]The E_a value was calculated in this work from viscosity−temperature data reported in ref 136.

relationship with viscosity (Table 6). Low-viscosity DESs such as CH_Cl + ethylene glycol also show very low E_a values, whereas the largest E_a values are obtained for highly viscous DESs, such as those containing sugar-based HBDs. Therefore, ion−HBD intermolecular interactions play a pivotal role in DES viscosity, while, as remarked by Florindo et al.,[118] the effects rising from the sizes of the ions are less important.

Bockris and co-workers reported a linear relationship between the activation energy for viscosity and the melting temperature for molten salts (E_a = 3.7RT_m).[155,156] Following this approach, Abbott et al.[114] showed an almost linear relationship between E_a and the DES melting point, although a reduced number of solvents was considered. Therefore, this behavior was analyzed in the present work for all of the DESs considered in Table 6, as shown in Figure 10. As a rule, the results in Figure 10 show that larger melting points lead to

Figure 10. Relationship between the activation energy for viscosity (E_a) and the melting temperature (T_m) for the DESs reported in Table 6. The solid line shows a linear fit (slope = 0.2043 kJ mol^{-1} K^{-1}, R^2 = 0.77). The green symbol shows the (0, 0) point, which was included in the fitting procedure following the behavior reported by Emi and Bockris[156] for molten salts.

larger viscosities (larger E_a), and this qualitative trend can be quantified because the results show a certain degree of linearity between the two properties. The constant of proportionality between E_a and T_m from the results reported in Figure 10 is 24.6 ± 3.3, which is in good agreement with the value reported by Abbott et al. for a reduced number of DESs (23.0) but lower than the value reported by Emi and Bockris[156] for molten salts (30.8). Nevertheless, this difference may arise from the aforementioned scatter in the DES viscosity data. Abbott and co-workers[115,157] analyzed the viscosity of DESs in the framework of hole theory, which was previously developed by Emi and Bockris[156] for molten salts and was also applied to ILs to analyze their viscosity.[158] In this theory, it is considered that the viscosity and electrical conductivity are correlated with the availability of holes in the fluid that allow suitable ionic motion, and thus, it considers that viscosity is mainly controlled by volumetric factors in spite of the strong intermolecular interactions developed in these systems. Therefore, although ion−HBD interactions play a pivotal role in determining the DES viscosity, steric effects should also play some role, which may be quantified by the hole theory approach. The distribution of holes $P(r)$ (i.e., the probability of finding a hole of radius r), in the corresponding DES (Figure 11) may be quantified from a simple expression, but it requires knowledge of the DES surface tension, which hinders its applicability because of the scarcity of these data. The distribution of hole sizes is dependent on the HBD type. For CH_Cl-based DESs the maxima of the distribution curves reported in Figure 1, r_{HOLES}, range from 1.17 to 1.42 Å for D-glucose and ethylene glycol, respectively. The type of salt also affects the distribution of hole sizes, as may be inferred from a comparison of the results for CH_Cl + glycerol and tetrapropylammonium bromide + glycerol DESs. Therefore, it seems that DESs containing larger holes lead to less viscous fluids, and although this is true for most of the studied DESs, the trend is not linear, as very viscous DESs such as CH_Cl + D-glucose deviate from the general trend (Figure 12a). It may be argued that the factor
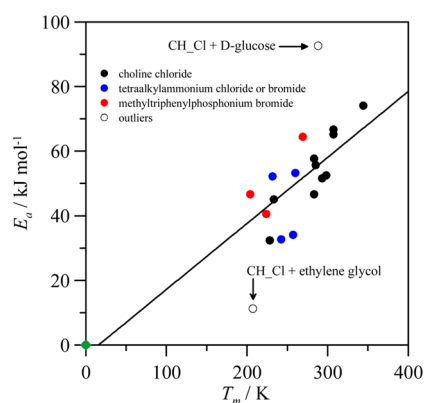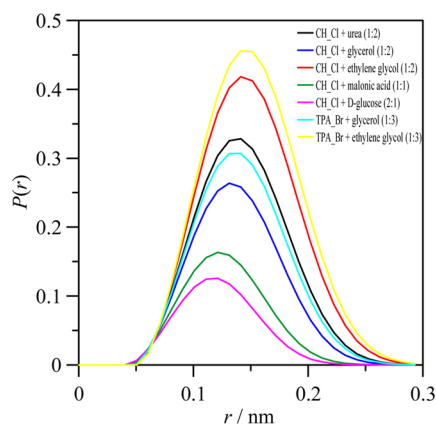
Figure 11. Distribution of hole sizes in selected DESs calculated according to hole theory. TPA_Br stands for tetrapropylammonium bromide. All of the values were calculated at 298.15 K from experimental data reported by D'Agostino et al.,[136] Jibril et al.,[125] and Hayyan et al.[122]

controlling the viscosity should be not only the size of available holes but also the size of the involved molecules, and thus, the ratio of the molecular radius (r_{DES}) to r_{HOLES} was calculated. In order to calculate the molecular radius of the corresponding DES, the hard-core volume of the optimized salt + HBD structure was calculated as reported in previous sections, and in a simplified approach, this hard-core volume was assigned to a sphere, from which r_{DES} was calculated. The results reported in Figure 12b show that the r_{DES}/r_{HOLES} ratio has an effect on the viscosity (the larger the ratio the larger the viscosity), and thus, the availability of holes of suitable size plays an important role in the viscous behavior of the DES. However, the additional effect of the strength of intermolecular forces between the HBD and the ions should also play a pivotal role.

The development of predictive viscosity models for DESs using approaches such as QSAR or group contribution methods, which have been used successfully for ILs, is absent in the literature, and therefore, systematic experimental and theoretical studies should be carried out to allow the advancement of theoretical modeling of DES dynamic properties.

Electrical Conductivity. This property is strongly correlated with viscosity: the larger the viscosity, the lower the

conductivity. Thus, most of the available DESs have very low conductivities (lower than 1 mS cm^{-1} at ambient temperature),[87] which can be a problem for certain electrochemical applications. Only low-viscosity DESs such as those containing ethylene glycol or imidazole with CH_Cl show large conductivities.[91,157]

The problems reported in the previous section regarding scatter and divergences in the literature data for viscosity are also inferred for conductivity, which is reasonable considering the close connection between these two properties (Table 7). These large divergences between literature sources, together with the scarcity of experimental data and the absence of systematic studies to identify the effects of the salt and HBD types on the conductivity, make additional studies of the electrochemical properties of DESs necessary.

The hole theory was also applied by Abbott et al.[157] to predict DES conductivity, and although good results were obtained in some cases (e.g., the CH_Cl + ethylene glycol 1:2 DES), poor predictions were reported for others (e.g., the CH_Cl + glycerol 1:2 DES). This shows that the ion mobility and thus conductivity are determined by not only the availability of suitable holes but also the type and strength of ion−HBD interactions. Likewise, it should be remarked that ions migrate while complexed with the corresponding HBD,[114] and thus, the size of the HBD determines the hydrodynamic radius of the migrating species, which should be taken into account for the calculation of transport properties.

It has been claimed[87] that the DES conductivity increases with increasing salt (IL) concentration, but this is not true for all DESs, and the variation of the conductivity with the salt concentration is dependent on both the type of salt and the HBD. This leads to systems in which the conductivity decreases with increasing salt concentration (e.g., tetrabutylammonium chloride + ethylene glycol) or systems in which the conductivity−salt concentration trend evolves through a maximum (e.g., CH_Cl + ethylene glycol), as shown in Figure 13.

The effect of temperature on conductivity is commonly described according to Arrhenius-type behavior.[94,113,114,117,125,145] This allows the calculation of the activation energy, which has been related with hole theory and the availability of free volume, leading to conclusions
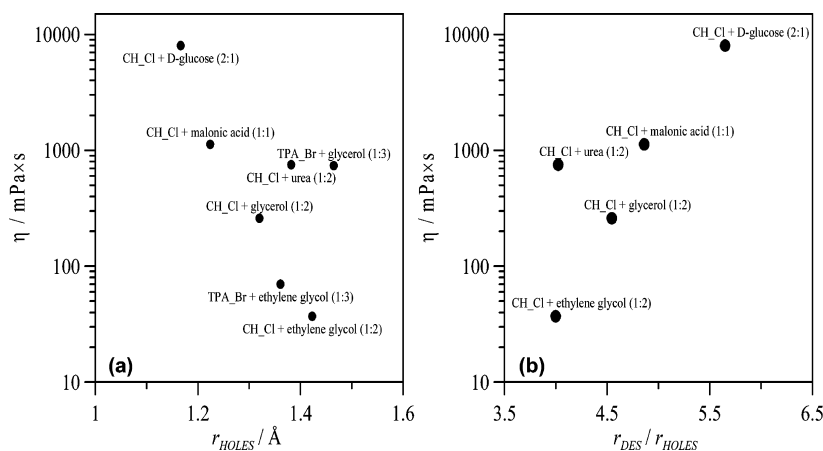

Figure 12. Relationships between the dynamic viscosity (η) and (a) the DES hole radius (r_{HOLES}) and (b) the ratio of the DES radius to hole radius (r_{DES}/r_{HOLES}). Viscosity data were taken from refs 122, 125, and 136.

Table 7. Comparison of Literature Sources for DES Conductivity (κ)

salt	HBD	salt:HBD molar ratio	T/K	κ/mS cm^{-1}	sample origin[a]	ref
choline chloride	urea	1:2	313.15	0.199	prepared	115
		1:2	303.15	2.31	commercial	159
choline chloride	glycerol	1:2	298.15	1.300[b]	prepared	113
		1:2	298.15	1.749	prepared	160
choline chloride	malonic acid	1:1	298.15	0.742[b]	prepared	114
		1:1	298.15	0.91	commercial	145

[a]The sample origin column shows whether the DES was prepared for the corresponding study by mixing the two components or purchased from a commercial supplier. [b]Obtained from graphical results.
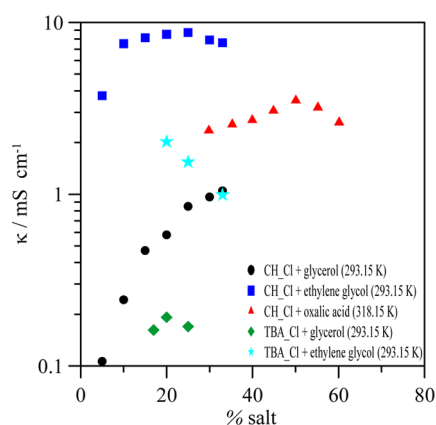

Figure 13. Plot of the effect of composition on the conductivity (κ) for salt + HBD DESs. Experimental data were taken from refs 114, 117, and 157. TBA_Cl stands for tetrabutylammonium chloride.

analogous to those reported in the previous section for viscosity.

The relationship between viscosity and conductivity is commonly analyzed in the literature using Walden plots, in which molar conductivity (Λ, calculated from conductivity and density) and fluidity (the inverse of viscosity) are plotted on log−log scales and compared with a so-called ideal line (obtained for a 0.01 M KCl aqueous solution, which has a slope equal to 1 and goes through the origin of coordinates).

Deviations from this ideal line are analyzed as a function of fluid ionicity and good or poor character for ILs.[68] A decrease in ionicity is defined in terms of deviations from the ideal line for ILs, with poor ILs defined as those that lie below the ideal line. Therefore, Walden plots have also been considered in the literature for analyzing the properties of DESs.[91,145,157] Literature results show that DESs present larger deviations from the ideal reference line than most ILs, which may be justified by considering that migrating species are ions for ILs and ions + HBD complexes for DESs.[68,157] Increasing ionicity is obtained with increasing salt concentration for DESs.[157] The effect of HBD type on the behavior of DESs with regard to the Walden rule is reported in Figure 14a for CH_Cl DESs. Low-viscosity DESs (e.g., those with ethylene glycol or 2,2,2-trifluoroacetamide) show lower ionicities, whereas very viscous ones lie closer to the ideal line. Thus, it could be inferred that HBDs that strongly interact with the corresponding ions lead to larger ionicities. The type of involved salt has also a large effect on the ionicity, as the results in Figure 14b for glycerol-containing DESs show that alkylammonium salts lead to liquids with poorer ionicity, whereas those containing phosphonium cations may be classified as good ILs. The anion involved in the salt also changes the DES ionicity, as shown by comparison of the tetrabutylammonium bromide and chloride results, with larger ionicities for chlorine-containing DES (Figure 14b).

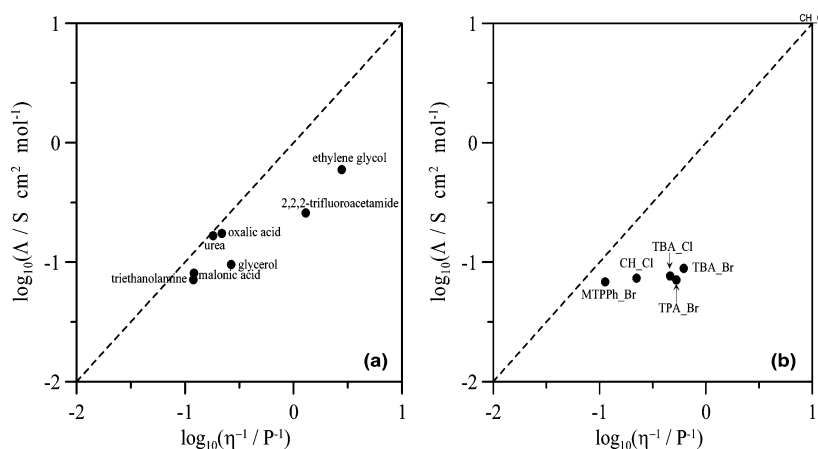The development of predictive methods for DES conductivity is very scarce in the literature. Ghareh-Bagh et al.[160]

Figure 14. Walden plots for DESs. The effect of the HBD for CH_Cl + HBD DESs is analyzed in panel (a), and the effect of salt type for salt + glycerol DESs is analyzed in panel (b). Experimental data were taken from (a) refs 145, 157, and 159 and (b) refs 94, 117, 125, 146, and 157. Panel (a): urea (1:2) at 303.15 K; glycerol (1:2) and ethylene glycol (1:2) at 293.15 K; and malonic acid (1:1), oxalic acid (1:1), 2,2,2-trifluoroacetamide (1:2), and ethanolamine (1:2) at 298.15 K. Panel (b): all at 318.15 K except CH_Cl DES (293.15 K); all at 1:3 molar ratio except MTPPh_Br (1:1.75). Molar conductivity (Λ) and fluidity (η^{-1}) are plotted logarithmically. Acronyms in panel (b): TPA_Br, tetrapropylammonium bromide; TBA_Br, tetrabutylammonium bromide; TBA_Cl, tetrabutylammonium chloride; MTPPh_Br, methyltriphenylphosphonium bromide. The dashed lines show the reference (so-called ideal) lines obtained for 0.01 M KCl aqueous solution.

Table 8. Surface Tension (γ) for Selected DESs

salt	HBD	salt:HBD molar ratio	T/K	γ/mN m^{-1}	ref
choline chloride	urea	1:2	298.15	52.0	136
choline chloride	glycerol	1:2	298.15	56.0	136
choline chloride	ethylene glycol	1:2	298.15	48.0	136
choline chloride	1,4-butanediol	1:3	298.15	47.17	83
choline chloride	malonic acid	1:1	298.15	65.7	136
choline chloride	phenylacetic acid	1:2	298.15	41.86	114
choline chloride	D-glucose	2:1	298.15	71.7	122
choline chloride	fructose	2:1	298.15	74.01	144
tetrapropylammonium bromide	glycerol	1:3	303.15	46	117
tetrapropylammonium bromide	ethylene glycol	1:3	303.15	40.1	117
tetrapropylammonium bromide	triethylene glycol	1:3	303.15	39.3	117
tetrabutylammonium chloride	glycerol	1:3	303.15	52.7	125
tetrabutylammonium chloride	ethylene glycol	1:3	303.15	46.2	125
tetrabutylammonium chloride	triethylene glycol	3:1	303.15	46.2	125
N,N-diethylethanolammonium chloride	glycerol	1:4	298.15	59.35	83
N,N-diethylethanolammonium chloride	ethylene glycol	1:3	298.15	47.51	83
N,N-diethylethanolammonium chloride	2,2,2-trifluoroacetamide	1:2	298.15	40.27	83
methyltriphenylphosphonium bromide	glycerol	1:3	298.15	58.94	83
methyltriphenylphosphonium bromide	ethylene glycol	1:4	298.15	51.29	83
methyltriphenylphosphonium bromide	triethylene glycol	1:5	298.15	49.85	83

developed an artificial neural network (ANN) approach for the electrical conductivity of ammonium- and phosphonium-based DESs leading to an absolute relative deviation of 4.4%, which may be considered as satisfactory. Nevertheless, the DESs studied by Ghareh-Bagh et al.[160] involved only three types of salts (CH_Cl, N,N-diethylethanolammonium chloride, and methyltriphenylphosphonium bromide) combined with two HBDs (glycerol and ethylene glycol), and although they analyzed the predictive ability of the model in the 298.15−353.15 K range, the number of studied DES was very limited. Thus, the approach should be tested using a larger database of DESs, which is not currently available in the literature.

The behavior of DESs with regard to viscosity and conductivity is strongly correlated with the ability of the involved molecules to move, and thus, the knowledge of self-diffusion coefficients may shed light on the nanoscopic behavior of DESs and its relationship to the transport properties. Nevertheless, in spite of its importance, measurements on self-diffusion coefficients (D) are extremely scarce in the literature, and only D'Agostino et al.[136] and Abbott et al.[113] have reported studies, both for CH_Cl-based DESs, using pulsed field gradient NMR methods. The results show D values following Arrhenius-type behavior with different activation energies for the cations and the HBDs (values for the anions were not reported because of experimental limitations, but they should be similar to those of HBDs since the anions migrate paired with the corresponding HBDs). Cations diffuse slower than HBDs for urea, glycerol, and ethylene glycol, whereas the opposite effect is obtained for malonic acid, which is justified by considering the formation of chains in malonic acid through hydrogen bonding.[136] The main conclusion from the D measurements is that although the role of the available hole size distribution in the transport mechanism is important, the role of intermolecular forces also must be considered. Molecules diffuse according to a hopping mechanism, in which the hole mobility plays a pivotal role.[113,136]

Interfacial Properties. These properties, in particular surface tension, are of remarkable importance for mass transfer purposes, but experimental data are still scarce (Table 8).

Surface tension is strongly dependent on the strength of intermolecular forces between the HBDs and the corresponding salt, and thus, highly viscous DESs (e.g., CH_Cl + ethylene glycol or tetraalkylammonium-based DESs) are fluids with high surface tension. The surface tension of DES is remarkably high for most of the studied systems, being larger than those of many ILs,[161] which is a measure of the strength of ion−HBD hydrogen bonding. The high surface tension of CH_Cl + malonic acid DES and also those for DESs containing sugars are also remarkable, and they point to large hydrogen-bonding networks in these fluids. The type of cation also has a large effect on the surface tension, as shown by the values for CH_Cl + glycerol in comparison with tetrapropyl- or tetrabutylammonium bromide/chloride + glycerol: the presence of hydroxyl groups in the cation leads to higher surface tension because of their hydrogen-bonding ability. Likewise, results for tetrapropyl- and tetrabutylammonium DESs show that increasing the cation alkyl chain length leads to higher surface tension. Moreover, the surface tension decreases with increasing temperature in a linear trend for all of the studied DESs,[83,90,113,117,125,144] and it also decreases with increasing salt mole fraction because of the weakening of the HBD hydrogen-bonding network upon mixing.[113]

Considering the relevance of surface tension, different property modeling approaches have been developed with predictive purposes, which should be considered with caution because of the small number of DESs for which experimental data are available for model validation purposes. Abbott and co-workers[113−115] used the surface tension data to calculate the availability of holes in the fluids in the framework of hole theory, which allowed an analysis of the fluids' viscosity as a function of the hole distribution as explained in the previous sections. Shahbaz et al.[83] developed a predictive approach for surface tension using the parachor parameter, in which a parachor for each molecular component of the DES was calculated using a group contribution approach and the parachor of the DES was calculated as the sum of those corresponding to the DES components weighted by the mole fractions. This approach led to very good predictive results for

Table 9. Refractive Index with Regard to the Sodium D Line (n_D) for Selected DESs

salt	HBD	salt:HBD molar ratio	T/K	n_D	ref
choline chloride	urea	1:2	303.15	1.5044	159
choline chloride	glycerol	1:2	298.15	1.48675	141
choline chloride	ethylene glycol	1:2	298.15	1.46823	141
choline chloride	glycolic acid	1:1	298.15	1.48293	118
choline chloride	oxalic acid	1:1	298.15	1.48649	118
choline chloride	malonic acid	1:1	298.15	1.48713	118
choline chloride	levulinic acid	1:2	298.15	1.46792	118
choline chloride	glutaric acid	1:1	298.15	1.48330	118
choline chloride	D-glucose	2:1	298.15	1.6669	122
choline chloride	fructose	2:1	298.15	1.5197	120
tetrapropylammonium bromide	glycerol	1:3	303.15	1.4858	117
tetrapropylammonium bromide	ethylene glycol	1:3	303.15	1.4717	117
tetrapropylammonium bromide	triethylene glycol	1:3	303.15	1.4732	117
tetrabutylammonium chloride	glycerol	1:3	303.15	1.4774	125
tetrabutylammonium chloride	ethylene glycol	1:3	303.15	1.4672	125
tetrabutylammonium chloride	triethylene glycol	3:1	303.15	1.4836	125
N,N-diethylethanolammonium chloride	glycerol	1:2	303.15	1.48435	152
N,N-diethylethanolammonium chloride	ethylene glycol	1:2	303.15	1.46768	152
methyltriphenylphosphonium bromide	glycerol	1:1.75	298.15	1.5666	94
methyltriphenylphosphonium bromide	ethylene glycol	1:4	288.15	1.5622	94
methyltriphenylphosphonium bromide	2,2,2-trifluoroacetamide	1:8	298.15	1.4849	94

DES parachors for the nine cholinium-, ammonium-, and phosphonium-based DESs. The main weakness of this approach is that obtaining surface tension data from the predicted parachors requires experimental density data, and thus, it may not be considered as a purely predictive method for surface tension. Shahbaz et al.[83] also used the Othmer equation to predict the surface tension of DESs. In this approach, critical properties of the DES are required, but these are not experimentally available and thus must be predicted using group contribution approaches. Although the average percent error for the nine studied DESs was 2.57%, the disagreements with experimental data increased with increasing temperature, and the model was not able to reproduce the rate of variation of surface tension with temperature.

Additional studies of other interfacial properties involving DESs are almost absent in the literature. The only one is by Abbott et al.,[140] who reported measurements of contact angles and coefficients of kinetic friction for CH_Cl + urea (1:2), + glycerol (1:2), + ethylene glycol (1:2), and + oxalic acid (1:1) DESs for metal surfaces such as Al, bronze, Cu, or steel in the framework of DESs as new lubricating agents for metal surfaces. The reported results for interfacial and tribological properties showed that DESs are suitable alternatives to traditional oils for lubricating iron-based metal surfaces but not for hydrophobic ones such as aluminum. The studies by Abbott et al.[140] also showed very low corrosion rates for CH_Cl-based DESs with regard to metal surfaces, which is highly surprising considering the presence of chlorine cation but may be justified by considering its interaction with the corresponding HBDs.

Polarity. The polarity of a fluid is a key property for characterizing its ability to dissolve solutes. In spite of this relevance, the available information on the polarity of DESs is almost null in the literature, which is a remarkable problem considering that DESs have been proposed as an environmentally friendly alternative to common volatile organic solvents. The usual way to measure solvent polarity is through the so-called solvatochromic parameters, which measure the hypsochromic (blue) shift or bathochromic (red) shift of UV−

vis bands for certain probes (dyes) as a function of solvent polarity.[162] Abbott et al.[113] characterized the solvent polarity of CH_Cl + glycerol at molar ratios of 1:1, 1:1:5, 1:2, and 1:3 using Reichardt's dye scale ($E_T(30)$ parameter)[162] and the Kamlet−Taft scale (π^*, α, and β parameters).[163] The measured $E_T(30)$ values show that these CH_Cl + glycerol DESs are polar fluids with polarities in the range of those for primary and secondary alkylammonium ILs.[164] These $E_T(30)$ values are similar to those of common polar HBD solvents, which may be justified by considering the hydroxyl groups of glycerol and the choline cation. The $E_T(30)$ values change with increasing CH_Cl from 57.17 kcal mol^{-1} for pure glycerol to 59 kcal mol^{-1} for pure CH_Cl (extrapolated) with an almost linear trend.

Pandey et al.[165] carried out a large experimental study on CH_Cl-based DESs using several solvatochromic probes. These authors discarded the use of the common Reichardt's betaine dye 30 to characterize the polarity of CH_Cl-based DESs because of protonation and solubility restrictions. Instead, they used the alternative betaine dye 33, from which the $E_T(30)$ parameter may be also calculated. Their studies of CH_Cl + urea (1:2), + glycerol (1:2), and + ethylene glycol (1:2) (malonic acid DESs could not be measured because of band assignment) confirmed that these are highly polar fluids. Pandey et al.[165] remarked that the polarity of these DESs is even higher than those of short-chain alcohols and most common ILs. The largest $E_T(30)$ values were obtained for glycerol DESs, followed by ethylene glycol and urea, which is attributed to the number of hydroxyl groups in the corresponding HBDs. Interestingly, these authors remarked that most of the DES polarity rises from the hydrogen-bonding ability of the involved HBDs, and thus, upon CH_Cl + HBD interactions a gain in dipolarity/polarizability is obtained, which is partially offset by a loss of hydrogen-donor ability in the DES because some of the HBD groups interact with the ion. Therefore, DES polarity can be fine-tuned through the selection of HBDs and tuning of the available HBD groups in the corresponding ions. Additional studies by Pandey et

al.[165] using fluorescence probes showed the prevailing role of the hydrogen-bonding ability of the involved HBD, leading to larger polarities for DESs containing glycerol and ethylene glycol (having hydroxyl groups) than those with malonic acid or urea (having carboxylic or amide groups).

Other Relevant Properties. Some studies have reported other physicochemical properties that are useful for characterizing DES behavior and applications. Refractive indices with regard to the sodium D line have been measured (Table 9) and have even been used to determine DES free volumes.[118] All of the reported DES have large refractive indices, in the same range as those of common ILs[166] (1.47 to 1.67 with an average value of 1.4990 ± 0.0473 for these DES reported in Table 9). The refractive indices are closely related to the electronic polarizabilities as reported by Seki et al.[166] for ILs, and thus, the most common DESs are highly polarizable media.

Studies of the thermal properties of DESs are required for applications such as heat transfer or thermal storage, but again, they are almost absent in the literature. Li and co-workers[167,168] reported measurements of the isobaric heat capacity (C_p) for CH_Cl + urea (1:2), + glycerol (1:2), and + ethylene glycol (1:2) and for N,N-diethylethanolammonium + glycerol (1:2) and + ethylene glycol (1:2). In the case of the CH_Cl-based DESs, the C_p values are in the order glycerol (237.7 J mol^{-1} K^{-1} at 303.15 K) > ethylene glycol (190.8 J mol^{-1} K^{-1} at 303.15 K) > urea (181.4 J mol^{-1} K^{-1} at 303.15 K), whereas larger values are obtained for the N,N-diethylethanolammonium-based DESs (250.4 and 204.1 J mol^{-1} K^{-1} at 303.15 K for glycerol and ethylene glycol, respectively). These C_p values and their evolution with the type of HBD and salt can be justified by considering the number of available translational, rotational, and vibrational degrees of freedom. ILs were proposed as alternative thermal storage materials because of their large thermal storage densities ($E_{thermal}$) in comparison with common oils, and therefore, $E_{thermal}$ may be calculated from the available density and C_p values and compared with those values for pure ILs.[149,169] For example, calculations for CH_Cl + ethylene glycol using C_p data from Leron and Li[167] leads to $E_{thermal}$ = 486.6 MJ m^{-3} (considering an output−input range of 200 K),[149] which is remarkably larger than the values for commonly used oils. Therefore, DESs could also be used as thermal storage materials having environmentally friendly properties, with their storage capacities being tuned through the selection of suitable salt−HBD combinations.

The thermal stability of choline-based DESs has been studied by Rengstl et al.,[170] who found that the decomposition temperatures are in the 269−280 °C range, which are higher than those of the pure ILs and HBDs. They are more than 250 °C higher than the melting points, thus leading to a large liquid range in which these DESs could be used for many technological applications.

Other studies have reported some useful properties such as speed of sound,[137] electrochemical behavior,[171] and moisture sorption ability (very remarkable for CH_Cl + levulinic acid DES),[119] but the number of studied DESs is very limited, and thus, it is not possible to draw systematic conclusions that may drive new research directions.

Computational Studies of DES Properties and Nanoscopic Structure. Studies using computational chemistry approaches have proved to be very useful for characterizing IL properties and features at the nanoscopic level and their connection with relevant macroscopic physicochemical properties.[172] Studies of CH_Cl + urea (1:2) have been reported by

Sun et al.,[173] Perkins et al.,[174,175] and Shah and Mjalli,[159] showing the strong hydrogen bonding between the urea amino group and the chloride anion with structural arrangements to maximize the number of hydrogen bonds between the HBD and the anion as the driving structural feature. To our knowledge, all of the molecular dynamics studies available in the literature are limited to the CH_Cl + urea DES, and thus, further systematic studies are required to determine the effect of the salt and HBD types on the nanoscopic features. Another very useful theoretical approach is density functional theory, but its suitability for DESs has only been considered by Zhang et al.[176] for a DES based on choline chloride + magnesium chloride hexahydrate.

3. CARBON DIOXIDE CAPTURE AND GAS SEPARATION

Acid Gas Removal and Gas Solubility in Ionic Liquids. Increasing energy demand in both industrial and residential areas is triggering increased usage of fossil-based fuels, which cause unprecedented fugitive and toxic gaseous emissions to the atmosphere. Release of these gases is harmful to the environment, especially CO_2, as it increases the acidity and salinity of fresh and sea/ocean water sources.[177] According to the latest figures published by the Intergovernmental Panel on Climate Change (IPCC), approximately 75% of the increase in atmospheric CO_2 is due to the amplified fossil-fuel-related activities.[178] Such greenhouse gas emissions are believed to increase the average global temperature, but more importantly, the recent CO_2 levels in the atmosphere were recorded at an all-time high of 400 ppm and were projected to reach 570 ppm in a recent study conducted by the IPCC.[179] This number would translate into an average global temperature increase of 1.9 °C, which in turn would have the effect of increasing sea level by approximately 3.8 m.[180] Besides CO_2, carbon monoxide (CO), nitrogen oxides (NO_2 and NO_3), sulfur dioxide (SO_2), mercury, and other particulates have severe environmental impact through the atmospheric emissions, and their effects were discussed in a recent study conducted by the Energy Information Administration (EIA).[181] Because of the increased global risk caused by the toxic emissions, several options have been considered in both political and academic platforms in order to find feasible and sustainable emission control models. Among those, (*i*) reducing energy intensity, (*ii*) reducing carbon intensity through carbon-free energy sources, and (*iii*) enhancing capture of toxic gas releases and improving sequestration technologies are considered as immediate action plans. Since the existing technologies for energy generation from renewable sources such as solar energy harvesting, wind energy utilization, etc., are not yet well-established, scientists are still trying to overcome the associated challenges in order to develop those technologies for mass applications. Increasing energy efficiency and using smart power grids are ongoing work that needs improvements in inter- and intranational energy and power transmission systems. The other option is to develop technologies to capture toxic gaseous emissions in more effective ways by using various chemicals and processes. When all three of the above-mentioned options are considered, seeking more effective gas capture solvents are the most realistic near-future tangible targets from both the academic and industrial points of view.

In particular, CO_2 capture contributes three-fourths of the overall gaseous emissions capture activity, and it has a cumulative negative cost side effect of a 50% increase in

electricity production in related industries.[182] There are various options and technologies such as absorption, adsorption, cryogenic capture processes, and membrane separation units that are currently used to manage CO_2 emissions. The choice of the suitable technology depends on the characteristics of the gas stream from which CO_2 will be captured. Such characteristics are heavily dependent on the type of dynamics of the process through which the fuel is processed and used. For instance, the flue gas characteristics are different when coal-fired power plants, natural-gas-fired power plants, the cement industry, and the aluminum industry are considered. Some of these processes use chemical-based separation methods, whereas other techniques use physical-based separation systems. The nature of the separation system is determined on the basis of the nature of the solvents or porous (solid-state) media.[183] Moreover, the location and condition of the process stream, such as pre- and post- combustion cases, and the chemical and physical requirements of the capture agents vary.

When the CO_2 capture process is considered, amine solvent-based technology has been in use for more than 70 years. Amines are chemicals that can be described as derivatives of ammonia in which one or more of the hydrogen atoms has been replaced by an alkyl or aryl group. Amines are classified as primary, secondary, or tertiary depending on whether one, two, or three of the hydrogen atoms of ammonia have been replaced by organic functional groups. Some of the amines most commonly used in CO_2 capture are monoethanolamine (MEA), methyldiethanolamine (MDEA), 2-amino-2-methyl-propanol (AMP), piperazine (PIPA), diglycolamine (DGA), diethanolamine (DEA), and diisopropanolamine (DIPA). The amine-based CO_2 capture process has been the most dominant acid gas removal technology since the early stages of the deployment of CO_2 management and mitigation programs, mostly because CO_2 recovery rates of up to 98% and product purities in excess of approximately 99% can be achieved. In recent years there have been some commercial patented products that have been very popular in the market for CO_2 scrubbing processes, such as Selexol and Rectisol.[184,185] However, there are questions about the amine process, including the loss of amine reagents and transfer of water into the gas stream during the desorption stage, chemical degradation to form corrosive byproducts, and high energy consumption during regeneration, as well as insufficient carbon dioxide/hydrogen sulfide capture capacity.[186]

In order to eliminate problematic sides of the amine process, both academia and industry have been researching substitute solvents that are chemically more robust, having high CO_2 affinity with viable thermophysical properties. In the beginning of the past decade, ILs have started to get great attention in academia, and one application field of ILs was testing their gas (including CO_2) uptake potential under various process conditions. Some recent works have shown that ILs are very promising alternative capture solvents, mostly for CO_2 and other toxic gases such as H_2S and SO_2 as well.[187−191] The physical and chemical properties of ILs at various temperatures (mostly at room temperature) can be adjusted through modification of their cationic and anionic moieties, allowing them to be tailored for various applications and process needs such as making solvents, solid-state photocells, and thermal and hydraulic fluid lubricants.[192−194] Bates et al.[187] attempted to modify the cation of imidazolium-based ILs through the attachment of a primary amine moiety, which subsequently has high affinity and can capture CO_2 through carbamate

formation. Therefore, the use of ILs for gas capture and in particular CO_2 capture has received interest in recent years because of their unique characteristics and high solubilities.[195,196] More specifically, by modification of solvent properties at room temperature through hydrogen-bond donors, IL mixtures may have great potential for efficient CO_2 absorption.[86]

Deep Eutectic Solvents and Gas Solubility Studies. As described above, the current state-of-the-art amine process has severe drawbacks in the CO_2 capture process. Many researchers have explored these facts, and new capture methods for efficient and environmentally viable alternatives have been tested for more than a couple of decades. Because of their extremely low vapor pressures, ILs have great potential to overcome the problematic high volatility of the amine process.[197] Additionally, because of their high thermal and chemical stability,[74,198] nonflammable nature, high solvation capacity, and promising gas solubility features, ILs have started to be among the main attractive chemical compounds for the past decade. Early works with ILs showed that cations and anions can increase the affinity for both CO_2 and SO_2 according to their choice and their tunability to synthesize task-specific solvents that can physically interact with the gas to be absorbed (mostly with CO_2)[190,199−201] through reversible binding. The initial experimental research, which was reported back in 1999[202] and then followed by the range of studies,[203−212] suggested that the nature of the anion plays the key and deterministic role in CO_2 solubility in the ILs. It was observed that the solubility of CO_2 in ILs containing nitrate anion is much less than that in ILs containing bis(trifluoromethylsulfonyl)imide anion.[213] It was later highlighted that fluorination on the anion or to a lesser extent on the cation increases the CO_2 solubility in an IL; however, such fluorination has a trade-off negative side effect in actual processes.[214] On the contrary, increasing the alkyl-chain length on the cation improves the CO_2 solubility, where a recent study has suggested that the solubility of CO_2 in ILs is mostly controlled by entropic effects.[215] Thus, the solubility of CO_2 in ILs at pressures up to 5 MPa and temperatures between 298 and 363 K falls with a common trend in molality versus pressure plots.[216]

Although the selectivity of CO_2 removal through ILs in both post- and precombustion gas streams is very high,[217] postcombustion gas capture and separation has the issue of low capacity.[218] Recent studies have shown that with 1-hexyl-3-methylpyridinium bis(trifluoromethylsulfonyl)imide, the selectivity of CO_2 over CH_4 is on the order of 10 at low to room temperatures.[203,217] The solubility of hydrocarbon gases such as methane is relatively higher[202,203] than the other toxic gases in the flue, pre- and postcombustion stages, such as SO_2 and H_2S.[219] Therefore, it could be concluded that the use of ILs has great potential for either sequential or simultaneous capture and scrubbing not only for CO_2 but also for SO_2 and H_2S.[220−223]

Despite all of the above-mentioned promising gas solubilities in ILs, they have not yet been proven to be alternative materials for large-scale industrial scrubbing agents for several reasons, such as low capacity,[218] toxicity,[53] and high synthesis cost.[116] Despite their fascinating functionalities, these materials still need huge capital investments for bulk production. Moisture sensitivity and nonbiodegradable functionality are additional issues that make them questionable for industrial applications, although they still remains as highly attractive chemical structures for academic purposes. In order to overcome these

Table 10. Summary of CO$_2$ and SO$_2$ Solubilities in DESs and in Some ILs for Comparison Purposes[a]

DES components						
IL	HBD	molar ratio	absorbate	solubility	T/P (K/bar)	ref
choline chloride	glycerol + DBN	1:2:6 CH_Cl:gly:DBN	CO$_2$	2.3–2.4 mmol/g	ambient	225
choline chloride	urea	1:2	CO$_2$	3.559 mmol/g	303.15/60	226
choline chloride	ethylene glycol	1:2	CO$_2$	3.1265 mmol/g	303.15/58.63	227
choline chloride	ethanolamine	1:6	CO$_2$	0.0749 mmol/g	298/10	228
MTPP_Br	ethanolamine		CO$_2$	0.0716 mmol/g	298/10	
TBA_Br	ethanolamine		CO$_2$	0.0591 mmol/g	298/10	
[BMIM][PF$_6$]	–	–	CO$_2$	0.200 mol/mol	298/12.99	204
[EMIM][BF$_4$]	–	–	CO$_2$	1.5999 mmol/g	298/41.55	229
choline chloride	triethylene glycol	4:1	CO$_2$	0.1941 mmol/g	293/5	230
choline chloride	phenol	4:1	CO$_2$	0.2108 mmol/g	293/5	
choline chloride	diethylene glycol	4:1	CO$_2$	0.1852 mol/mol	293/5	
choline chloride	glycerol	1:1	SO$_2$	0.678 g/g	290/1	231
[DMEA][glutarate] (2:1)	–	–	SO$_2$	0.623 mol/mol	313/0.004	232
CPL	KSCN	3:1	SO$_2$	1.38 mol/mol	313/1	233
acetamide	KSCN	3:1	SO$_2$	0.588 g/g	293/1	
acetamide	NH$_4$SCN	3:1		0.579 g/g	293/1	
CPL	NH$_4$SCN	3:1	SO$_2$	0.559 mol/mol	293/1	
urea	NH$_4$SCN	3:2	SO$_2$	0.372 mol/mol	303.1	
triethylene glycol (PEG150)	DBU	1:1	CO$_2$	1.04 mol/mol	298/1.0	234
[bmim][Tf$_2$N]	DBU	1:1	CO$_2$	1.0 mol/mol	298/1.0	235
[N$_{2224}$][CA]	H$_2$O	1:n	CO$_2$	0.66 mol/mol	298/4.4	236
choline chloride	glycerol	1:2	CO$_2$	3.692 mol/kg	303/58	237
[CPL][TBAB]		1:1	SO$_2$	0.680 mol/mol	298/1	238
[CPL][TBAB] + H$_2$O		1:1:4	SO$_2$	0.52 g/g	293/1.0	239
CPL−acetamide		1:1	SO$_2$	0.497 g/g	303/1	240
CPL−imidazole		1:1	SO$_2$	0.624 g/g	300/1	
[HMIM][Tf$_2$N]	–	–	SO$_2$	0.844 mol/mol	298/2.94	220
[hmpy][Tf$_2$N]	–	–	SO$_2$	0.844 mol/mol	298/2.96	
choline chloride	2,3-butanediol	1:4	CO$_2$	0.0188 mol/mol	298/5.08	241
choline chloride	1,4-butanediol	1:3	CO$_2$	0.0164 mol/mol	298/5.09	
choline chloride	1,2-propanediol	1:3	CO$_2$	0.0165 mol/mol	298/5.14	
choline chloride	lactic acid	1:2	CO$_2$	0.0248 mol/mol	348/19.27	242
choline chloride	urea	1:1.5	CO$_2$	0.201 mol/mol	313.15/118.4	243
choline chloride	urea	1:2	CO$_2$	0.309 mol/mol	313.15/1125	
choline chloride	urea	1:2.5	CO$_2$	0.203 mol/mol	313.15/1145	
choline chloride	urea + H$_2$O	50 wt % CH_Cl + urea (reline) + 50% H$_2$O	CO$_2$	0.111 mol/mol	313/7.8	244
choline chloride	urea + H$_2$O	60 wt % reline + 40% H$_2$O	CO$_2$	0.103 mol/mol	313/8.06	
choline chloride	urea + H$_2$O	70 wt % rel + 30% H$_2$O	CO$_2$	0.097 mol/mol	313/8.09	
choline chloride	urea + H$_2$O + MEA	50 wt % reline + 15 wt % MEA + H$_2$O	CO$_2$	0.229 mol/mol	313/8.18	
choline chloride	urea + H$_2$O + MEA	60 wt % reline + 10 wt % MEA + H$_2$O	CO$_2$	0.202 mol/mol	313/8.25	
choline chloride	urea + H$_2$O + MEA	70 wt % reline + 5 wt % MEA + H$_2$O	CO$_2$	0.189 mol/mol	313/8.13	

[a]Acronyms: CH_Cl, choline chloride; DBN, 1,5-diazabicyclo[4.3.0]non-5-ene; MTPP_Br, methyltriphenylphosphonium bromide; TBA_Br, tetrabutylammonium bromide; [BMIM][PF$_6$], 1-butyl-3-methylimidazolium hexafluorophosphate; [EMIM][BF$_4$], 1-ethyl-3-methylimidazolium tetrafluoroborate; [DMEA][glutarate], dimethylethanolammonium glutarate; CPL, caprolactam; DBU, diazabicyclo[5.4.0]undec-7-ene; [bmim]-[Tf$_2$N], 3-butyl-1-methylimidazolium bis(trifluoromethanesulfonyl)amide; [N$_{2224}$][CA], triethylbutylammonium carboxylate; [CPL][TBAB], caprolactam tetrabutylammonium bromide; [HMIM][Tf$_2$N], 1-n-hexyl-3-methylimidazolium bis(trifluoromethylsulfonyl)imide; [hmpy][Tf$_2$N], 1-n-hexyl-3-methylpyridinium bis(trifluoromethylsulfonyl)imide.

negative aspects of ILs and utilize their chemical flexibility, recently emerging materials called deep eutectic solvents have been developed as versatile alternatives.[90,113,224] Mixing two or three components capable of intermolecular interactions through hydrogen bonding generates DESs, which have depressed freezing points[86] and other eutectic physical properties that lie well below those of each of the individual constituents of the mixture.[113] Some of the recent research findings on the solubilities of flue gases, particularly CO$_2$ and SO$_2$, are summarized in Table 10. Florindo et al.[118] have recently prepared DESs based on choline chloride and carboxylic acids that could have negligible toxicity and lower cost of preparation.

DESs share many unusual characteristics of ILs[87] such as negligible vapor pressure, low volatility, wide liquid range, high thermal and chemical stability, nonflammability, and high solvation capacity. Moreover, unlike ILs, DES compounds are easy to prepare in high purity, and the choice of additional solvent helps to fine-tune and produce DES compounds to have considerable low cost, less or even no toxicity, and biodegradable structure.[114,245]

Because of the above-mentioned advantageous features, the potential use of DESs in various applications has started to be exploited and extensively explored. Recent studies have shown the application of these novel solvents in various applications such as electrochemical processes, metal electrodeposition, electropolishing, and electroplating.[245−248] Additionally, DESs have also been characterized and proposed for other chemical processes, including biological applications such as biocatalytic reactions,[249,250] biodiesel production,[113,251,252] and drug solubilization[96] as well as chemical reactions such as organic material syntheses.[88] From a materials science point of view, their thermal and physicochemical properties have also been characterized in some recent works.[141,167]

Deep Eutectic Solvents and CO_2 Systems. In order to substitute amine-based CO_2 capture systems, many different techniques and materials have been developed over the past few years, including recently explored materials such as ILs and DESs. ILs have been used, followed by the use of DESs, since the latter have excellent tunable properties and can be adjusted for improved CO_2 solubility. Open literature in this area has focused mostly on the systems that contain choline chloride ILs; however, some other IL families have been also investigated for tackling the problems associated with applications of DESs as gas absorbents. Wang et al.[253] used imidazolium-based ILs and superbase mixtures to develop IL- and DES-based CO_2 scrubbing systems. This study highlighted the effect of the superbase, as it would abstract the weakly acidic proton from the imidazolium cation to improve the CO_2 affinity, which subsequently increases CO_2 capture. In another study, Wang et al.[235] showed that a 1:1 molar ratio of an IL + alcohol group system and a superbase can reversibly capture up to 1 mol of CO_2 per mole of superbase used. It was concluded that the anion superbases in anion-functionalized protic ILs deprotonate weak proton donors (e.g., alcohols and phenols), resulting in a reaction and capture of CO_2. Additionally, an attempt was made to tune the CO_2 absorption enthalpy through phosphonium hydroxide to neutralize weak proton donors with different acidities,[254] which may effectively increase the CO_2 uptake by DES mixed superbase systems. Similarly, Yang et al.[255] recently worked on tailor-made IL systems including amino-functionalized and superbase-derived protic ILs for CO_2 capture applications. This research group showed some DES applications formed with polyethylene glycol and an amidine or guanidine superbase system for efficient CO_2 capture up to 1.0 mol/mol.[234]

Li et al.[243] recently studied the solubility of CO_2 in DES systems formed with choline chloride and urea at different molar ratios at various pressures and temperatures. It was found that the solubility of CO_2 (x_{CO_2}) in choline chloride and urea DESs depends on three factors:

(i) The solubility of CO_2 increases with pressure and is more sensitive to the pressure in the low-pressure range.

(ii) The solubility of CO_2 decreases with increasing temperature whatever the pressure.

iii) The choline chloride:urea molar ratio has a significant effect on x_{CO_2} (e.g., at fixed pressure and temperature, a choline chloride + urea (1:2 molar ratio) DES exhibits higher CO_2 solubility than those with 1:1.5 and 1:2.5 molar ratios).

The DES prepared from choline chloride and urea with a 1:2 molar mixing ratio, known as reline, is reported to have the lowest melting point.[159] Reline has been termed as

hygroscopic,[159] since most of the choline chloride-based DESs always contain trace amounts of water, which may affect the hydrogen-bonding interactions and consequently modify their physical and chemical properties. For example, the densities of the DESs and their aqueous mixtures made of choline chloride and ethylene glycol in a 1:2 ratio have been found to decrease with increasing temperature and to increase with increasing pressure in the high range of 1−500 bar. This effects of temperature and pressure on the density of DES were attributed to the dependence of the hydrogen bonding on temperature and the decrease in the molecular distance and free volume of the mixture.[147] An earlier finding[154] revealed that water molecules in DES can act as an antisolvent and can prohibit CO_2 absorption. This hygroscopic behavior of DES significantly affects the solubility of CO_2 at low pressure and has been termed as a limitation of these mixtures.[244] As shown in Table 10, the solubility of CO_2 at different temperatures and CO_2 partial pressures decreases with increasing water content in the DES system composed of choline chloride and urea in a 1:2 molar ratio. Detailed investigations by Sun et al.[154] have demonstrated that the absorption of CO_2 turns from endothermic to exothermic at water concentrations below a molar ratio of 0.231. This finding could be an important benchmark as long as the swing absorption−stripping process for capturing CO_2 is concerned in the DES-based system. However, Wang et al.[236] demonstrated that the fast absorption of CO_2 in the DES derived from triethylbutylammonium carboxylate and water at room temperature and low pressure can be attributed mainly to the carboxylate anions rather than the interactions between cations and water molecules. It was further suggested that a long monocarboxylate chain would favor enlarged CO_2 solubility because of the availability of free volume between the anions, whereas the interaction of multiple carbonyl groups would affect the CO_2 affinity, resulting in lower CO_2 absorption.[236]

The effects of temperature and pressure[227,237] on the solubility of CO_2 in choline chloride-based DES mixtures were investigated over the temperature range of 303.15−343.15 K and pressures up to 6 MPa. Figure 15 obtained from literature data[237] demonstrates that the solubility of CO_2 in the CH_Cl + glycerol DES system with a component molar ratio
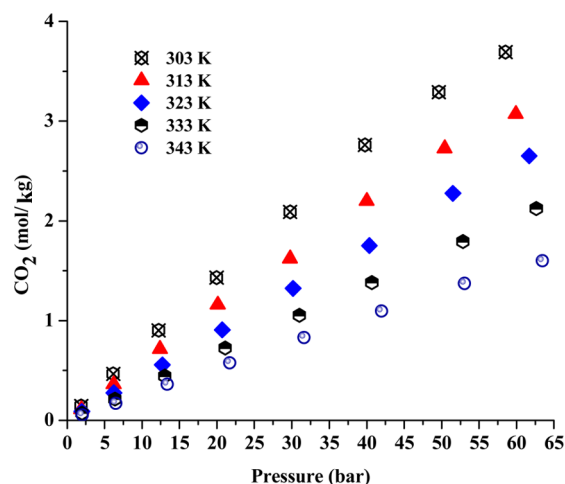

Figure 15. Effect of temperature and pressure on the solubility of CO_2 in the DES based on choline chloride and glycerol in a 1:2 molar ratio. The data were obtained from the literature.[237]
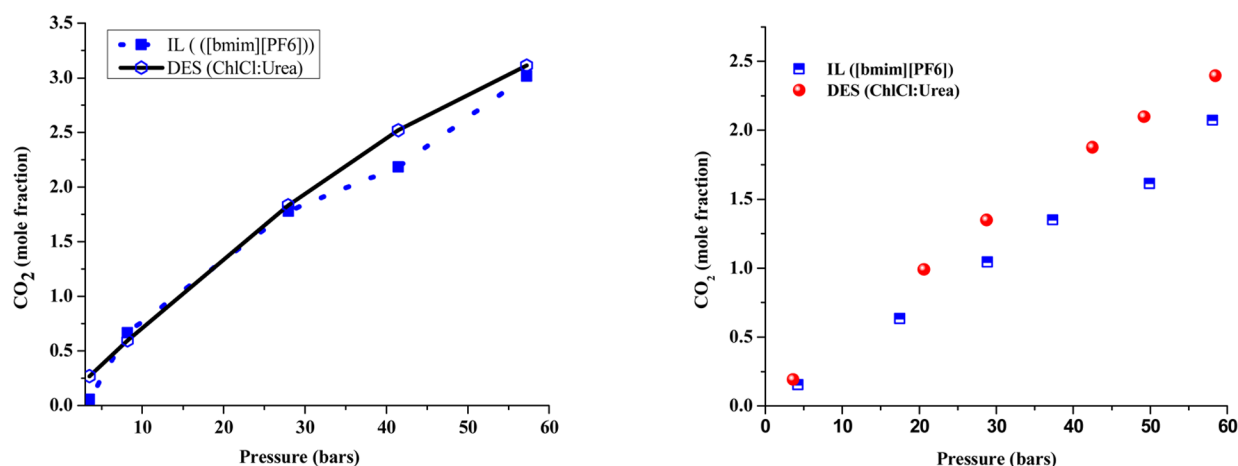
Figure 16. Comparison of CO_2 solubilities in the $[bmim][PF_6]$ ILs and the CH_Cl + urea DES system: (left) experiments at 298 K and 60 bar;[214,226] (right) experiments at 313 K (red circles) and 333 K (blue squares) and pressures of up to 60 bar. Data were taken from refs 208 and 243.

of 1:2 increases linearly with pressure and decreases with increasing temperature, and the extended Henry's law equation was found to be a function of temperature and pressure with an average absolute deviation of 1.6%. Various other studies[226,227,242,243] (Table 10) have also found similar effects of reduction and enhancement of the CO_2 solubility in DESs with increasing temperature and pressure, respectively. Li et al.[243] further stated that increasing the choline chloride:urea molar ratio from 1:1.5 to 1:2 and 1:2.5 has no significant effect on the CO_2 capture by these mixtures. However, the dissolved CO_2 mole fraction in the liquid DES system ranged from a low value of 0.032 for CH_Cl:urea = 1:2.5 at 333.15 K and 1.08 MPa to 0.309 for CH_Cl:urea = 1:2 at 313.15 K and 12.5 MPa.

In order to develop an environmentally friendly and biorenewable solvent, Francisco et al.[242] coupled choline chloride with an organic acid (lactic acid) in a 1:2 ratio and explored a novel DES compound for CO_2 capture that has a low transition temperature and tunable physical and chemical properties. Although the low-transition-temperature mixtures prepared by Francisco et al.[242] have excellent thermophysical properties, they have lower CO_2 absorption capacities than the common ILs. Nevertheless, the solubility of CO_2 in DESs prepared from the combination of choline chloride with urea and ethylene glycol have shown promising results compared with imidazolium-based DES systems.[190]

In view of the above discussion, it can be concluded that the DES made of choline chloride and urea with a molar ratio of 1:2 has shown the best performance to date, with a measured CO_2 uptake of 3.559 mmol/g at 303.15 K and 60 bar. However, this value is comparatively lower than the 4.52 mol of CO_2/kg withheld by sulfonate ILs at 307 K and 80 bar.[256] However, at room temperature and atmospheric pressure, choline chloride mixed with glycerol in a molar ratio of 1:1 has the largest CO_2 uptake to date, 0.678 g/g, which can be compared to 0.28 mol/mol absorbed by monoethanolamine-modified room temperature ILs at 298 K and 10 bar.[257] This clearly indicates that DESs can absorb more CO_2 than the toxic ILs on the basis of their tunable physical and chemical properties. Nevertheless, detailed investigations are highly recommended to determine the mechanism of CO_2 absorption by DESs and to further elaborate whether it depends on the free volume and/or on the strength of intermolecular and intramolecular interactions and to what extent the CO_2 solubility can be tuned within these novel solvent systems.

Figure 16 shows a comparison of pure IL and DES systems and their comparative CO_2 solubility performances under similar pressure and temperature conditions. It can be seen from these works that DES systems perform better in CO_2 capture when similar pure IL systems are considered.

Deep Eutectic Solvents and SO$_2$ Systems. Besides the absorption of CO_2, DESs have been investigated for the capture of various other gases such as SO_2,[231] H_2, CO, and methane. However, these studies are very limited, and there is a strong need for experimental studies to establish a database on the behavior of DESs in coexistence with SO_2. As one of the main air contaminants, like CO_2, SO_2 is emitted from the burning of fossil fuels and has extremely harmful effects on human health and environment due to the formation of acid rain.[258] The classical approach for managing SO_2 emissions is flue gas desulfurization (FGD) technology, such as wet or dry FGD processes.[259−261] Like CO_2 capture studies, most of the current SO_2 capture technologies that use DES systems are focused on the utilization of choline chloride as the IL, since these materials are very economical, biodegradable, and nontoxic and either can be extracted from biomass or are readily available as bulk commodity chemicals. Although enough literature is available on the absorption of SO_2 by various types of ILs, it is generally understood that ILs have the issue of thermal instability[262] and are not suggested as the best alternatives to the commonly available technologies. Recent findings have revealed that tuning the electronegativity of nitrile-containing anion-functionalized ILs with imidazolium cations may enhance SO_2 absorption; however, the maximum amount absorbed with this toxic IL was only 1.13 g/g.[263]

On the other hand, recent research[231] has shown that nontoxic DES systems composed of choline chloride and glycerol with a 1:1 molar mixing ratio can absorb up to 0.678 g of SO_2/g at room temperature. As shown in Table 11, further investigation revealed that increasing the glycerol mole fraction in the mixture affects the SO_2 solubility, which decreases to 0.320 g/g for the molar mixing ratio of 1:4. Temperature and pressure effects on the SO_2 absorption performance were also studied, and the results indicated that the solubility of SO_2 in the DES decreases continuously with increasing temperature and increases with increasing partial pressure. The observed solubility of SO_2 in the DES system with a 1:1 molar mixing ratio decreased from 0.678 g/g at 20 °C to 0.158 g/g at 80 °C and increased continuously from 0.153 to 0.678 g/g as the SO_2

Table 11. Solubilities of SO₂ (in g/g of DES) in Choline Chloride + Glycerol DES Systems with Various Molar Mixing Ratios at 1 atm at Different Experimental Temperatures

$T/°C$	1:1	1:2	1:3	1:4
20	0.678	0.482	0.380	0.320
30	0.514	0.348	0.270	0.225
40	0.394	0.256	0.195	0.162
50	0.309	0.192	0.143	0.118
60	0.245	0.148	0.109	0.090
70	0.195	0.119	0.089	0.070
80	0.158	0.091	0.066	0.055

partial pressure increased from 0.1 to 1.0 atm. These results suggested that most of the absorbed SO₂ could be easily released by heating the DES, while low temperature is favorable for effective SO₂ absorption.

Although the cation of the IL makes the major contribution to the solubility process, unlike the case of CO₂,[215] the length of the alkyl chains has no obvious effect on the solubility of SO₂ in imidazolium-based ILs with lactate anion.[262] Additionally, increasing the lactam cation in caprolactam (CPL) tetrabutylammonium bromide (TBAB) ILs also affects the SO₂ absorption, since enhancement of the CPL:TBAB molar ratio decreases the solubility.[238]

Guo et al. prepared economically and environmentally benign DES systems with different molar ratios of CPL and TBAB and tested these new materials for SO₂ capture at various temperatures and atmospheric pressure.[238] As shown in Figure 17, the equilibrium solubilities of SO₂ in these different
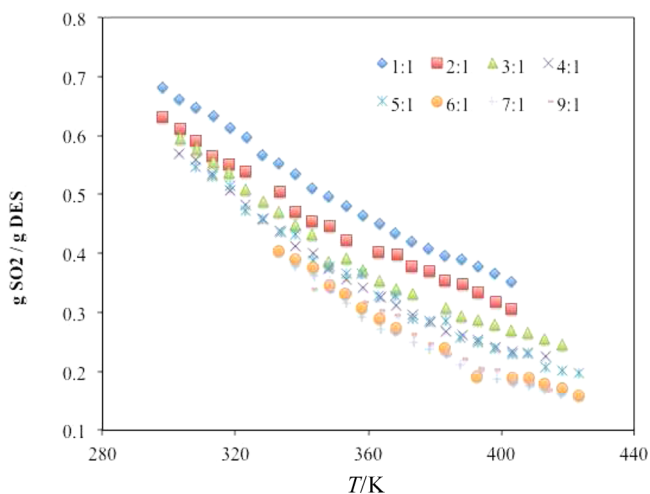

Figure 17. Solubility of SO₂ as a function of temperature in [CPL][TBAB] with different molar mixing ratios of caprolactam and tetrabutylammonium bromide.[238]

mixtures showed a strong dependence on the temperature and molar ratio of the parent chemicals at atmospheric pressure. It was found that the mole-fraction solubility of SO₂ decreases significantly both with increasing temperature (at the given molar ratio) and increasing mole fraction of CPL in [CPL][TBAB] at a given temperature. The maximum solubility observed for [CPL][TBAB] with a molar mixing ratio of 1:1 was 0.680 g/g at 298.2 K, whereas it was reduced to 0.351 g/g at 373.2 K at constant atmospheric pressure.

Almost similar results of decreasing SO₂ absorption with increasing temperature were observed by Liu et al.[240] when different CPL-based eutectic solvents obtained from low-molecular-weight organic compounds (such as acetamide, imidazole, furoic acid, benzoic acid, o-toluic acid) were tested for SO₂ solubility at atmospheric pressure. This decrease in the solubility was attributed to the escape of SO₂ molecules from the solution due to the breakdown of intermolecular bonds, which was subsequently caused by the higher temperature.[239] It is worth mentioning here that absorption amounts (Table 10) in CPL and amine-based DES systems were higher than those of CPL and acid-based DES systems, since the solubility of SO₂ in CPL–imidazole was 0.624 g/g, while it was 0.497 g/g for CPL–acetamide under similar conditions of temperature, pressure, and molar ratio. Liu et al.[233] studied CPL–KSCN with a molar mixing ratio of 3:1, which showed excellent performance by absorbing 0.618 g of SO₂/g at 313 K and 1 bar, while acetamide–KSCN (3:1) captured 0.588 g/g.

The strong appearance of hysteresis, change in the DES color, and shifting of NH absorption peaks from 12.05 ppm for the original CPL–imidazole to 10.23 ppm after SO₂ absorption suggested chemisorption in the case of CPL–imidazole. However, CPL–acetamide showed excellent reversible cycles of absorption–desorption with no hysteresis and no color change, suggesting physical absorption of SO₂.[240] Duan et al.[239] attempted to modify the viscosity of [CPL][TBAB] with the addition of water to further increase the solubility and affinity of SO₂ in this binary mixture. However, mixing water with [CPL][TBAB] minimizes the viscosity, but it further reduces the SO₂ capturing capacity of [CPL][TBAB]:H₂O. Upon heating of this densest phase, SO₂ can be removed easily, and the materials can be reused for absorption. Huang et al.[232] prepared three hybrid solvents of hydroxylammonium carboxylates by mixing water with dimethylethanolammonium (DMEA) and three different dicarboxylates (glutarate, malate, and malonate) to capture SO₂ at low and moderate pressures. It was found that the 2:1 [DMEA][glutarate] mixture has high alkalinity and can absorb more SO₂ than the rest of the mixtures. Although the effect of water on the SO₂ solubility was not mentioned clearly, the higher and faster absorption at low pressure was mainly attributed to chemical absorption, whereas the isotherm at moderate pressure represented Langmuir-type characteristics, indicating physical absorption of SO₂ as well.

Additionally, Figure 18 shows a comparison of SO₂ solubilities in some selected ILs and the CH_Cl + glycerol DES system. When the SO₂ solubility performance is considered, the pure ILs outperformed the DES system. Therefore, it can be concluded from the above discussion that DESs may have excellent potential to be considered both for the low- and high-pressure CO₂ capture and limited potential for SO₂ absorption for both pre- and postcombustion processes. Most of their properties can be tuned according to the working demands by choosing the proper components and ratio. Literature studied to date regarding the parameters influencing the solubility of CO₂ and SO₂ in eutectic solvents confirmed that at constant pressure the solubility decreases with increasing temperature and increases with increasing pressure at constant temperature. The solvent composition and mixture ratio also contribute to the absorption capacity irrespective of the synthesis procedure. Further investigations are still needed to determine the effect of water on the affinity and capturing capacity, the absorption behavior (chemical,
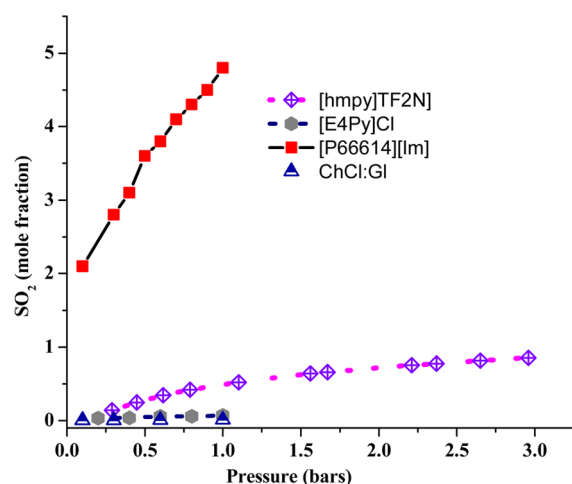
Figure 18. Solubilities of SO_2 in various ILs (1-hexyl-3-methylimidazolium bis(trifluoromethylsulfonyl)imide, 1-[2-(2-methoxyethoxy)-ethyl]pyridinium chloride, and an azole-based IL) and a CH_Cl + glycerol DES.[220,232,264−267]

physical, or both), reusability of the solvents, the real cost of the materials, and regeneration of the absorbed gases.

4. CONCLUSIONS

This review summarizes the state of the art on the knowledge of physicochemical properties of DESs and their application for gas absorption purposes, with special attention to carbon capture operations. The available studies on this new type of solvent are centered on DESs based on choline chloride, with scarce studies on DESs developed around other types of compounds. The experimental studies on DES physicochemical properties are scarce, with serious divergences among data obtained from different literature sources. Likewise, it should be remarked that there is an absence of systematic studies to determine the effects of salt and hydrogen-bond-donor type and the molar ratio in the mixture on the solvent properties. Moreover, studies at high pressure are almost negligible. The available literature on gas solubility studies is limited to CO_2 and minor studies on SO_2, but studies on carbon capture from complex gas mixtures such as flue gases or selectivity studies are absent. The scarcity of molecular modeling studies that would reveal the nanoscopic mechanisms controlling their physicochemical properties and gas solubility trends hinders the development of suitable structure−property relationships. Moreover, systematic physicochemical studies of suitable groups of DESs using samples with well-known purity and accurate measurement methods are also required for reliable process design purposes and fluid characterization. Nevertheless, the available literature information shows that these fluids are a suitable alternative platform to ILs for technological applications such as carbon capture, as the possibility of tailoring their properties through the judicious selection of salts, hydrogen-bond donors, and molar ratios would allow the development a large amount of sorbents with lower cost and better physicochemical properties than many ILs.

ASSOCIATED CONTENT

Supporting Information

DESs selected for QSAR modeling of DES melting points and melting point QSAR modeling results (Tables S1−S3). This

material is available free of charge via the Internet at http://pubs.acs.org.

AUTHOR INFORMATION

Corresponding Authors
*E-mail: sapar@ubu.es (Santiago Aparicio).
*E-mail: mert.atilhan@qu.edu.qa (Mert Atilhan).

Notes
Disclaimer: The statements made herein are solely the responsibility of the authors.
The authors declare no competing financial interest.

REFERENCES

(1) Climate Change 2013: The Physical Science Basis. Contribution of Working Group I to the Fifth Assessment Report of the Intergovernmental Panel on Climate Change; Stocker, T. F., Qin, D., Plattner, G. K., Tignor, M. M. B., Allen, S. K., Boschung, J., Nauels, A., Xia, Y., Bex, V., Midgley, P. M., Eds.; Cambridge University Press: Cambridge, U.K., 2013.

(2) Lacis, A. A.; Schmidt, G. A.; Rind, D.; Ruedy, R. A. Atmospheric CO_2: principal control knob governing earth's temperature. Science 2010, 330, 356−359.

(3) Meinshausen, M.; Smith, S. J.; Calvin, K.; Daniel, J. S.; Kainuma, M. L. T.; Lamarque, J. F.; Matsumoto, K.; Montzka, S. A.; Raper, S. C. B.; Riahi, K.; Thomson, A.; Velders, G. J. M.; van Vuuren, D. P. P. The RCP greenhouse gas concentrations and their extensions from 1765 to 2300. Clim. Change 2011, 109, 213−241.

(4) Friedlingtein, P.; Andrew, R. N.; Rogelj, J.; Peters, G. P.; Canadell, J. G.; Knutti, R.; Luderer, G.; Raupach, M. R.; Schaeffer, M.; van Vuuren, D. P.; Le Quéré, C. Persistent growth of CO_2 emissions and implications for reaching climate targets. Nat. Geosci. 2014, 7, 709−715.

(5) Kriegler, E.; Weyant, J. P.; Blanford, G. J.; Krey, V.; Clarke, L.; Edmonds, J.; Fawcett, A.; Luderer, G.; Riahi, K.; Richels, R.; Rose, S. K.; Tavoni, M.; van Vuuren, D. P. The role of technology for achieving climate policy objectives: overview of the EMF 27 study on global technology and climate policy strategies. Clim. Change 2014, 123, 353−367.

(6) van Vliet, J.; Hof, A. F.; Mendoza, A.; van der Berg, M.; Deetman, S.; den Elzen, M. G. J.; Lucas, P. L.; van Vuuren, D. P. Clim. Change 2014, 123, 559−569.

(7) Le Quéré, C.; Andres, R. J.; Boden, T.; Conway, T.; Houghton, R. A.; House, J. I.; Marland, G.; Peters, G. P.; van der Werf, G. R.; Ahlström, A.; Andrew, R. M.; Bopp, L.; Canadell, J. G.; Ciais, P.; Doney, S. C.; Enright, C.; Friedlingstein, P.; Huntingford, C.; Jain, A. K.; Jourdain, C.; Kato, E.; Keeling, R. F.; Klein, K.; Levis, S.; Levy, P.; Lomas, M.; Poulter, B.; Raupach, M. R.; Schwinger, J.; Sitch, S.; Stocker, B. D.; Viovy, N.; Zaehle, S.; Zeng, N. The global carbon budget 1959−2011. Earth Syst. Sci. Data 2013, 5, 165−185.

(8) Muradov, N. Liberating Energy from Carbon: Introduction to Decarbonization; Springer: New York, 2014.

(9) IPCC Special Report on Renewable Energy Sources and Climate Change Mitigation; Edenhofer, O., Pichs-Madruga, R., Sokona, Y., Seyboth, K., Matschoss, P., Kadner, S., Zwickel, T., Eickemeier, P., Hansen, G., Schlömer, S., von Stechow, C., Eds.; Cambridge University Press: Cambridge, U.K., 2011.

(10) Manzano, F.; Alcalde, A.; Montoya, F. G.; Zapata, A.; Gil, C. Scientific production of renewable energies worldwide: an overview. *Renewable Sustainable Energy Rev.* **2013**, *18*, 134−143.

(11) *World Energy Outlook 2013*; International Energy Agency: Paris, 2013.

(12) *Annual Energy Outlook 2014*; U.S. Energy Information Administration: Washington, D.C., 2014.

(13) Höök, M.; Tang, X. Depletion of fossil fuels and anthropogenic climate change. A review. *Energy Policy* **2013**, *52*, 797−809.

(14) *IPCC Special Report on Carbon Dioxide Capture and Storage*; Metz, B., Davidson, O., de Coninck, H., Loos, M., Meyer, L., Eds.; Cambridge University Press: Cambridge, U.K., 2005.

(15) Luderer, G.; Bosetti, V.; Jakob, M.; Leimbach, M.; Steckel, J. C.; Waisman, H.; Edenhofer, O. *Clim. Change* **2012**, *114*, 9−37.

(16) Friedman, S. J. CO$_2$ capture and sequestration. In *Fossil Energy*; Malhotra, R., Ed.; Springer: Menlo Park, CA, 2013; Chapter 16.

(17) Figueroa, J. D.; Fout, T.; Plasynski, S.; McIlvried, H.; Srivastava, R. D. Advances in CO$_2$ capture technology. The US Department of Energy's carbon sequestration program. *Int. J. Greenhouse Gas Control* **2008**, *2*, 9−20.

(18) D'Alessandro, D.; Smit, B.; Long, J. R. Carbon dioxide capture: prospects for new materials. *Angew. Chem., Int. Ed.* **2010**, *49*, 6058−6082.

(19) Jones, C. W. CO$_2$ capture from dilute gases as a component of modern global carbon management. *Annu. Rev. Chem. Biochem. Eng.* **2011**, *2*, 31−52.

(20) Pires, J. C. M.; Martins, F. G.; Alvim, M. C. M. Recent developments on carbon capture and storage: an overview. *Chem. Eng. Res. Des.* **2011**, *89*, 1446−1460.

(21) Li, B.; Duan, Y.; Luebke, D.; Morreale, B. Advances in CO$_2$ capture technology. *Appl. Energy* **2013**, *102*, 1439−1447.

(22) Boot-Handford, M. E.; Abanades, J. C.; Anthony, E. J.; Blunt, M. J.; Brandani, S.; MacDowell, N.; Fernández, J. R.; Ferrari, M.-C.; Gross, R.; Hallett, J. P.; Haszeldine, R. S.; Heptonstall, P.; Lyngfelt, A.; Makuch, Z.; Mangano, E.; Porter, R. T. J.; Pourkashanian, M.; Rochelle, G. T.; Shah, N.; Yao, J. G.; Fennell, P. S. Carbon capture and storage. *Energy Environ. Sci.* **2014**, *7*, 130−189.

(23) Wang, M.; Lawal, A.; Stephenson, P.; Sidders, J.; Ramshaw, C. Post-combustion CO$_2$ capture with chemical absorption: a state-of-the-art review. *Chem. Eng. Res. Des.* **2011**, *89*, 1609−1624.

(24) Lucquiaud, M.; Gibbins, J. Effective retrofitting of post-combustion CO$_2$ capture to coal-fired power plants and insensitivity of CO$_2$ abatement costs to base plant efficiency. *Int. J. Greenhouse Gas Control* **2011**, *5*, 427−438.

(25) Zhao, M.; Minett, A. I.; Harris, A. T. A review of techno-economic models for the retrofitting of conventional pulverised-coal power plants for post-combustion capture (PCC) of CO$_2$. *Energy Environ. Sci.* **2013**, *6*, 25−40.

(26) Davison, J. Performance and costs of power plants with capture and storage of CO$_2$. *Energy* **2007**, *32*, 1163−1176.

(27) Rochelle, G. T. Amine scrubbing for CO$_2$ capture. *Science* **2009**, *325*, 1652−1654.

(28) Gouedard, C.; Picq, D.; Launay, F.; Carrette, P. L. Amine degradation in CO$_2$ capture. I. A review. *Int. J. Greenhouse Gas Control* **2012**, *10*, 244−270.

(29) Raymal, L.; Bouillon, P. A.; Gomez, A.; Broutinn, P. From MEA to demixing solvents and future steps, a roadmap for lowering the cost of post-combustion carbon capture. *Chem. Eng. J.* **2011**, *171*, 742−752.

(30) Chi, S.; Rochelle, G. T. Oxidative degradation of monoethanol-amine. *Ind. Eng. Chem. Res.* **2002**, *41*, 4178−4186.

(31) Kittel, J.; Idem, R.; Gelowitz, D.; Tontiwachwuthikul, P.; Parrain, J.; Bonneau, A. Corrosion in MEA units for CO$_2$ capture. *Energy Procedia* **2009**, *1*, 791−797.

(32) Abu-Zahra, M. R. M.; Niederer, J. P. M.; Feron, P. H. M.; Versteeg, G. F. CO$_2$ capture from power plants: Part II. A parametric study of the economical performance on mono-ethanolamine. *Int. J. Greenhouse Gas Control* **2007**, *1*, 135−142.

(33) Romeo, L. M.; Bolea, I.; Escosa, J. M. Integration of power plant and amine scrubbing to reduce CO$_2$ capture costs. *Appl. Therm. Eng.* **2008**, *28*, 1039−1046.

(34) Rao, A. B.; Rubin, E. S. A technical, economic, and environmental assessment of amine-based CO$_2$ capture technology for power plant greenhouse gas control. *Environ. Sci. Technol.* **2002**, *36*, 4467−4475.

(35) Rao, A. B.; Rubin, E. S. Identifying cost-effective CO$_2$ control levels for amine-based CO$_2$ capture systems. *Ind. Eng. Chem. Res.* **2006**, *45*, 2421−2429.

(36) Bhown, A. S.; Freeman, B. C. Analysis and status of post-combustion carbon dioxide capture technologies. *Environ. Sci. Technol.* **2011**, *45*, 8624−8632.

(37) Husebye, J.; Brunsvold, A. L.; Roussanaly, S.; Zhang, X. Techno economic evaluation of amine based CO$_2$ capture: impact of CO$_2$ concentration and steam supply. *Energy Procedia* **2012**, *23*, 381−390.

(38) Lepaumier, H.; Picq, D.; Carrette, P. L. New amines for CO$_2$ capture. I. Mechanism of amine degradation in the presence of CO$_2$. *Ind. Eng. Chem. Res.* **2009**, *48*, 9061−9067.

(39) Chowdhury, F. A.; Okabe, H.; Yamada, H.; Onoda, M.; Fujioka, Y. Synthesis and selection of hindered new amine absorbents for CO$_2$ capture. *Energy Procedia* **2011**, *4*, 201−208.

(40) Dubois, L.; Thomas, D. Screening of aqueous amine-based solvents for post-combustion CO$_2$ capture by chemical absorption. *Chem. Eng. Technol.* **2012**, *35*, 513−524.

(41) Chowdury, F. A.; Yamada, H.; Higashii, T.; Goto, K.; Onoda, M. CO$_2$ capture by tertiary amine absorbents: a performance comparison study. *Ind. Eng. Chem. Res.* **2013**, *52*, 8323−8331.

(42) Porcheron, F.; Jacquin, M.; El-Hadri, N.; Saldana, D. A.; Goulon, A.; Faraj, A. Graph machine based-QSAR approach for modeling thermodynamic properties of amines: application to CO$_2$ capture in postcombustion. *Oil Gas Sci. Technol.* **2013**, *68*, 469−486.

(43) Wang, Q.; Luo, J.; Borgna, A. CO$_2$ capture by solid absorbents and their applications: current status and trends. *Energy Environ. Sci.* **2011**, *4*, 42−55.

(44) Sumida, K.; Rogow, D. L.; Mason, J. A.; McDonald, T. M.; Bloch, E. D.; Herm, Z. R.; Bae, T. H.; Long, J. R. Carbon dioxide capture in metal−organic frameworks. *Chem. Rev.* **2012**, *112*, 724−781.

(45) Samanta, A.; Zhao, A.; Shimizu, G. K. H.; Sarkar, P.; Gupta, R. Post-combustion CO$_2$ capture using solid sorbents: a review. *Ind. Eng. Chem. Res.* **2012**, *51*, 1438−1463.

(46) Hornboster, M. D.; Bao, J.; Krishnan, G.; Nagar, A.; Jayaweera, I.; Kobayashi, T.; Sanjurjo, A.; Sweeney, J.; Carruthers, D.; Petruska, M. A.; Dubois, L. Characteristics of an advanced carbon sorbent for CO$_2$ capture. *Carbon* **2013**, *56*, 77−85.

(47) Pera-Titus, M. Porous inorganic membranes for CO$_2$ capture: present and prospects. *Chem. Rev.* **2014**, *114*, 1413−1492.

(48) Karadas, F.; Atilhan, M.; Aparicio, S. Review on the use of ionic liquids (ILs) as alternative fluids for CO$_2$ capture and natural gas sweetening. *Energy Fuels* **2010**, *24*, 5817−5828.

(49) Brennecke, J. F.; Gurkan, B. E. Ionic liquids for CO$_2$ capture and emission reduction. *J. Phys. Chem. Lett.* **2010**, *1*, 3459−3464.

(50) Rees, N. V.; Compton, R. G. Electrochemical CO$_2$ sequestration in ionic liquids; a perspective. *Energy Environ. Sci.* **2011**, *4*, 403−408.

(51) Zhao, Z.; Dong, H.; Zhang, X. The research program of CO$_2$ capture with ionic liquids. *Chin. J. Chem. Eng.* **2012**, *20*, 120−129.

(52) Zhang, X.; Zhang, X.; Dong, H.; Zhao, Z.; Zhang, S.; Huang, Y. Carbon capture with ionic liquids: overview and progress. *Energy Environ. Sci.* **2012**, *5*, 6668−6681.

(53) Ramdin, M.; de Loos, T. W.; Vlugt, T. J. H. State-of-the-art of CO$_2$ capture with ionic liquids. *Ind. Eng. Chem. Res.* **2012**, *51*, 8149−8177.

(54) Wang, C.; Luo, X.; Zhu, X.; Cui, G.; Jiang, D.; Deng, D.; Li, H.; Dai, S. The strategies for improving carbon dioxide chemisorption by functionalized ionic liquids. *RSC Adv.* **2013**, *3*, 15518−15527.

(55) Lei, Z.; Dai, C.; Chen, B. Gas solubility in ionic liquids. *Chem. Rev.* **2014**, *114*, 1289−1326.

(56) Earle, M. J.; Seddon, K. R. Ionic liquids. Green solvents for the future. *Pure Appl. Chem.* **2000**, *72*, 1391−1398.

(57) Aparicio, S.; Alcalde, R. The green solvent ethyl lactate: an experimental and theoretical characterization. *Green Chem.* **2009**, *11*, 65−78.

(58) Paiva, A.; Caraverio, R.; Aroso, I.; Martings, M.; Reis, R. L.; Duarte, A. R. C. Natural deep eutectic solvents—Solvents for the 21st century. *ACS Sustainable Chem. Eng.* **2014**, *2*, 1063−1071.

(59) Plechkova, N. V.; Seddon, K. R. Applications of ionic liquids in the chemical industry. *Chem. Soc. Rev.* **2008**, *37*, 123−150.

(60) MacFarlane, D.; Tachikawa, N.; Forsyth, M.; Pringle, J. M.; Howlett, P. C.; Elliott, G. D.; Davis, J. H.; Watanabe, M.; Simon, P.; Angell, C. A. Energy applications of ionic liquids. *Energy Environ. Sci.* **2014**, *7*, 232−250.

(61) Aparicio, S.; Atilhan, M.; Karadas, F. Thermophysical properties of pure ionic liquids: review of present situation. *Ind. Eng. Chem. Res.* **2010**, *49*, 9580−9595.

(62) Torimoto, T.; Tsuda, T.; Okazaki, K.; Kuwataba, S. New frontiers in material science opened by ionic liquids. *Adv. Mater.* **2010**, *22*, 1196−1221.

(63) Niedermeyer, H.; Ashworth, C.; Brandt, A.; Welton, T.; Hunt, P. A. A step towards the a priori design of ionic liquids. *Phys. Chem. Chem. Phys.* **2013**, *15*, 11566−11578.

(64) Ventura, S. P. M.; Goncalves, A. M. M.; Sintra, T.; Pereira, J. L.; Goncalves, F.; Coutinho, J. A. P. Designing ionic liquids: the chemical structure role in the toxicity. *Ecotoxicology* **2013**, *22*, 1−12.

(65) Gierrnoth, R. Task specific ionic liquids. *Angew. Chem., Int. Ed.* **2010**, *49*, 2834−2839.

(66) Somers, A. E.; Howlett, P. C.; MacFarlane, D. R.; Forsyth, M. A review of ionic liquid lubricants. *Lubricants* **2013**, *1*, 3−21.

(67) Hallett, J. P.; Welton, T. Room-temperature ionic liquids: solvents for synthesis and catalysis. *Chem. Rev.* **2011**, *111*, 3508−3576.

(68) Le Bideau, J.; Viau, L.; Vioux, A. Ionogels, ionic liquid based hybrid materials. *Chem. Soc. Rev.* **2011**, *40*, 907−925.

(69) Wang, H.; Gurau, G.; Rogers, R. D. Ionic liquids processing of cellulose. *Chem. Soc. Rev.* **2012**, *41*, 1519−1537.

(70) Yasuda, T.; Watanabe, M. Protic ionic liquids: fuel cell applications. *MRS Bull.* **2013**, *38*, 560−566.

(71) Marrucho, I. M.; Brnaco, L. C.; Rebelo, L. P. N. Ionic liquids in pharmaceutical applications. *Annu. Rev. Chem. Biomol. Eng.* **2014**, *5*, 527−546.

(72) Emel'yanenko, V.; Boeck, G.; Verevkin, S. P. Volatile times for the very first ionic liquid: understanding the vapor pressures and enthalpies of vaporization of ethylammonium nitrate. *Chem.—Eur. J.* **2014**, *20*, 11640−11645.

(73) Meine, N.; Benedito, F.; Rinaldi, R. Thermal stability of ionic liquids assessed by potentiometric titration. *Green Chem.* **2010**, *12*, 1711−1714.

(74) Maton, C.; De Vos, N.; Stevens, C. V. Ionic liquid thermal stabilities: decomposition mechanism and analysis tools. *Chem. Soc. Rev.* **2013**, *42*, 5963−5977.

(75) Fox, D. M.; Gilman, J. W.; Morgan, A. B.; Shields, J. R.; Maupin, P. H.; Lyon, R. E.; De Long, H. C.; Trulove, P. C. Flammability and thermal characteristics characterization of imidazolium-based ionic liquids. *Ind. Eng. Chem. Res.* **2008**, *47*, 6327−6332.

(76) Biczak, R.; Pawlowska, B.; Balczewski, P.; Rychter, P. The role of the anion in the toxicity of imidazolium ionic liquids. *J. Hazard. Mater.* **2014**, *274*, 181−190.

(77) Pham, T. P. T.; Cho, C. W.; Yun, Y. S. Environmental fate and toxicity of ionic liquids: a review. *Water Res.* **2010**, *44*, 352−372.

(78) Peric, B.; Sierra, J.; Martí, E.; Cruañas, R.; Garau, M. A.; Arning, J.; Bottin-Weber, U.; Stolte, S. (Eco)toxicity and biodegradability of selected protic and aprotic ionic liquids. *J. Hazard. Mater.* **2013**, *261*, 99−105.

(79) Smiglak, M.; Reichert, W. M.; Holbrey, J. D.; Wilkes, J. S.; Sun, L.; Thrasher, J. S.; Kirichenko, K.; Sinngh, S.; Katritzky, A. R.; Rogers, R. D. Combustible ionic liquids by design: is laboratory safety another ionic liquid myth? *Chem. Commun.* **2006**, 2554−2556.

(80) Paduszynski, K.; Dománska, U. Viscosity of ionic liquids: an extensive database and a new group contribution model based on a feed-forwards artificial neural network. *J. Chem. Inf. Model.* **2014**, *54*, 1311−1324.

(81) Chen, L.; Sharifzadeh, M.; MacDowell, N.; Welton, T.; Shah, N.; Hallett, J. P. Inexpensive ionic liquids: $[HSO_4]^-$-based solvent production at bulk scale. *Green Chem.* **2014**, *16*, 3098−3106.

(82) Petkovic, M.; Seddon, K. R.; Rebelo, L. P. N.; Silva-Pereira, C. Ionic liquids: a pathway to environmental acceptability. *Chem. Soc. Rev.* **2011**, *40*, 1383−1403.

(83) Ventura, S. P. M.; Silva, F.; Goncalves, A. M. M.; Pereira, J. L.; Goncalves, F.; Coutinho, J. A. P. Ecotoxicity analysis of cholinium-based ionic liquids to *Vibrio fischeri* marine bacteria. *Ecotoxicol. Environ. Saf.* **2014**, *102*, 48−54.

(84) Hou, X. D.; Liu, Q. P.; Smith, T. J.; Li, N.; Zong, M. H. Evaluation of toxicity of cholinium amino acids ionic liquids. *PLoS One* **2013**, *8*, No. e59145.

(85) Asumana, C.; Yu, G.; Li, X.; Zhao, J.; Liu, G.; Chen, X. Extractive desulfurization of fuel oils with low-viscosity dicyanamide-based ionic liquids. *Green Chem.* **2010**, *12*, 2030−2037.

(86) Abbott, A. P.; Capper, G.; Davies, D. L.; Rasheed, R. K.; Tambyrajah, V. Novel solvent properties of choline chloride/urea mixtures. *Chem. Commun.* **2003**, 70−71.

(87) Zhang, Q.; Vigier, K. O.; Royer, S.; Jérôme, F. Deep eutectic solvents: synthesis, properties and applications. *Chem. Soc. Rev.* **2012**, *41*, 7108−7146.

(88) Carriazo, D.; Serrano, M. C.; Gutiérrez, M. C.; Ferrer, M. L.; del Monte, F. Deep eutectic solvents playing multiple roles in the synthesis of polymers and related materials. *Chem. Soc. Rev.* **2012**, *41*, 4996−5014.

(89) Wagle, D. V.; Zhao, H.; Baker, G. A. Deep eutectic solvents: sustainable media for nanoscale and functional materials. *Acc. Chem. Res.* **2014**, *47*, 2299−2308.

(90) Francisco, M.; Van Den Bruinhorst, A.; Kroon, M. C. Low transition temperature nixtures (LTTMs): a new generation of designer solvents. *Angew. Chem., Int. Ed.* **2013**, *52*, 3074−3085.

(91) Hou, Y.; Gu, Y.; Zhang, S.; Yang, F.; Ding, H.; Shan, Y. Novel binary eutectic mixtures based on imidazole. *J. Mol. Liq.* **2008**, *143*, 154−159.

(92) Shahbaz, K.; Baroutian, S.; Majalli, F. S.; Hashim, M. A.; AlNashef, I. M. Densities of ammonium and phosphonium based deep eutectic solvents: prediction using artifical intelligence and group contribution techniques. *Thermochim. Acta* **2012**, *527*, 59−66.

(93) Ghareh Bagh, F. S.; Mjalli, F. S.; Hashim, M. A.; Hadj-Kali, M. K. O.; AlNashef, I. M. Solubility of sodium salts in ammonium-based deep eutectic solvents. *J. Chem. Eng. Data* **2013**, *58*, 2154−2162.

(94) Kareem, M. A.; Mjalli, F. S.; Hashim, M. A.; Alnashef, I. M. Phosphonium based ionic liquid analogues and their physical properties. *J. Chem. Eng. Data* **2010**, *55*, 4632−4637.

(95) Hayyan, A.; Hashim, M. A.; Mjjalli, F. S.; Hayyan, M.; Alnashed, I. M. A novel phosphonium-based deep eutectic catalyst for biodiesel production from industrial low grade crude palm oil. *Chem. Eng. Sci.* **2013**, *92*, 81−88.

(96) Morrison, H. G.; Sun, C. C.; Neervannan, S. Characterization of thermal behavior of deep eutectic solvents and their potential as drug solubilization vehicles. *Int. J. Pharm.* **2009**, *378*, 136−139.

(97) Singh, B. S.; Lobo, H. R.; Shankarling, G. S. Choline chloride based eutectic solvents: magical catalytic system for carbon−carbon bond formation in the rapid synthesis of *β*-hydroxy functionalized derivatives. *Catal. Commun.* **2012**, *24*, 70−74.

(98) Hayyan, M.; Hashim, M. A.; Hayyan, A.; Al-Saadi, M. A.; Al-Nasher, I. M.; Mirghani, M. E. S.; Saheed, O. K. Are deep eutectic solvents benign or toxic? *Chemosphere* **2013**, *90*, 2193−2195.

(99) Singh, B.; Lobo, H.; Shankarling, G. Selective N-alkylation of aromatic primary amines catalyzed by bio-catalyst or deep eutectic solvent. *Catal. Lett.* **2011**, *141*, 178−182.

(100) Tang, B.; Row, K. H. Recent developments in deep eutectic solvents in chemical sciences. *Monatsh. Chem.* **2013**, *144*, 1427−1454.

(101) Choi, Y. H.; van Spronsen, J.; Dai, Y. T.; Vermerne, M.; Hollmann, F.; Arends, I. W. C. E.; Witkamp, G. J.; Verpoorte, R. Are natural deep eutectic solvents the missing link in understanding cellular metabolism and physiology? *Plant. Physiol.* **2011**, *156*, 1701–1705.

(102) Dai, Y.; van Spronsen, J.; Witkamp, G. J.; Verpoorte, R.; Choi, Y. H. Natural deep eutectic solvents as new potential media for green technology. *Anal. Chim. Acta* **2013**, *766*, 61–68.

(103) Chen, Y.; Cao, Y.; Sun, X.; Yan, C.; Mu, T. New criteria combined of efficiency, greenness, and economy for screening ionic liquids for CO$_2$ capture. *Int. J. Greenhouse Gas Control* **2013**, *16*, 13–20.

(104) Zhang, L. L.; Wang, J. X.; Liu, Z. P.; Lu, Y.; Chu, G. W.; Wang, W. C.; Chen, J. F. Efficient capture of carbon dioxide with novel mass-transfer intensification device using ionic liquids. *AIChE J.* **2013**, *59*, 2957–2965.

(105) Tomé, L. L.; Patinha, D. J. S.; Freire, C. S. R.; Rebelo, L. P. N.; Marrucho, I. N. CO$_2$ separation applying ionic liquid mixtures: the effect of mixing different anions on gas permeation through supported ionic liquid membranes. *RSC Adv.* **2013**, *3*, 12220–12229.

(106) Huang, Y.; Zhang, X.; Zhang, X.; Dong, H.; Zhang, S. Thermodynamic modeling and assessment of ionic liquid-based CO$_2$ capture processes. *Ind. Eng. Chem. Res.* **2014**, *53*, 11805–11817.

(107) Chong, F. K.; Eljack, F. T.; Atilhan, M.; Foo, D. C. Y.; Chemmangattuvalappil, N. G. Ionic liquid design for enhanced carbon dioxide capture—A computer aided molecular design approach. *Chem. Eng. Trans.* **2014**, *39*, 253–258.

(108) Moganty, S. S.; Chinthamanipeta, P. S.; Vendra, V. K.; Krishnan, S.; Baltus, R. E. Structure–property relationships in transport and thermodynamics properties of imidazolium bistriflamide ionic liquids for CO$_2$ capture. *Chem. Eng. J.* **2014**, *250*, 377–389.

(109) Letcher, T. M. *Chemical Thermodynamics for Industry*; Royal Society of Chemistry: Cambridge, U.K., 2004.

(110) Franca, J. M. P.; Nieto de Castro, C. A.; Matos, M.; Nunes, V. Influence of thermophysical properties of ionic liquids in chemical process design. *J. Chem. Eng. Data* **2009**, *54*, 2569–2575.

(111) Liu, Y. T.; Chen, Y. A.; Xing, Y. J. Synthesis and characterization of novel ternary deep eutectic solvents. *Chin. Chem. Lett.* **2014**, *25*, 104–106.

(112) Shabaz, K.; Mjalli, F. S.; Hashim, M. A.; Al-Nashef, I. M. Using deep eutectic solvents for the removal of glycerol from palm-oil based biodiesel. *J. Appl. Sci.* **2010**, *10*, 3349–3354.

(113) Abbott, A. P.; Harris, R. C.; Ryder, K. S.; D'Agostino, C.; Gladden, L. F.; Mantle, M. D. Glycerol eutectics as sustainable solvent systems. *Green Chem.* **2011**, *13*, 82–90.

(114) Abbott, A. P.; Boothby, D.; Capper, G.; Davies, D. L.; Rasheed, R. K. Deep eutectic solvents formed between choline chloride and carboxylic acids: versatile alternatives to ionic liquids. *J. Am. Chem. Soc.* **2004**, *126*, 9142–9147.

(115) Abbott, A. P.; Capper, G.; Gray, S. Design of improved deep eutectic solvents using hole theory. *ChemPhysChem* **2006**, *7*, 803–806.

(116) Francisco, M.; van der Bruinhorst, A.; Kroon, M. C. New natural and renewable low transition temperature mixtures (LTTMs): screening as solvents for lignocellulosic biomass processing. *Green Chem.* **2012**, *14*, 2153–2157.

(117) Mjalli, F. S.; Naser, J.; Jibril, B.; Alizadeh, V.; Gano, Z. Tetrabutylammonium chloride based ionic liquid analogues and their physical properties. *J. Chem. Eng. Data* **2014**, *59*, 2242–2251.

(118) Florindo, C.; Oliveira, F. S.; Rebelo, L. P. N.; Fernandes, A. M.; Marrucho, I. M. Insights into the synthesis and properties of deep eutectic solvents based on cholinium chloride and carboxylic acids. *ACS Sustainable Chem. Eng.* **2014**, *2*, 2416–2425.

(119) Maugeri, Z.; Domínguez, P. Novel choline-chloride-based deep-eutectic-solvents with renewable hydrogen bond donors: levulinic acid and sugar-based polyols. *RSC Adv.* **2012**, *2*, 421–425.

(120) Hayyan, A.; Mjalli, F. S.; AlNashef, I. M.; Al-Wahaibi, T.; Al-Wahaibi, Y.; Ali-Hashim, M. Fruit sugar-based deep eutectic solvents and their physical properties. *Thermochim. Acta* **2012**, *541*, 70–75.

(121) Shabaz, K.; Mjalli, F. S.; Hashim, M. A.; AlNashef, I. M. Using deep eutectic solvents based on methyl triphenyl phosphonium bromide for the removal of glycerol from palm-oil-based biodiesel. *Energy Fuels* **2011**, *25*, 2671–2678.

(122) Hayyan, A.; Mjalli, F. S.; AlNashef, I. M.; Al-Wahaibi, Y. M.; Al-Wahaibi, T.; Ali-Hashim, M. Glucose-based deep eutectic solvents: physical properties. *J. Mol. Liq.* **2013**, *178*, 137–141.

(123) Guo, W.; Hou, Y.; Ren, S.; Tian, S.; Wu, W. Formation of deep eutectic solvents by phenols and choline chloride and their physical properties. *J. Chem. Eng. Data* **2013**, *58*, 866–872.

(124) Abbott, A. P.; Capper, G.; Davies, D. L.; Rasheed, R. Ionic liquid based metal halide/substituted quaternary ammonium salt mixtures. *Inorg. Chem.* **2004**, *43*, 3447–3452.

(125) Jibril, B.; Mjalli, F.; Naser, J.; Gano, Z. New tetrapropylammonium bromide-based deep eutectic solvents: synthesis and characterizations. *J. Mol. Liq.* **2014**, *199*, 462–469.

(126) Zhao, H.; Baker, G. A.; Holmes, S. New eutectic ionic liquids for lipase activation and enzymatic preparation of biodiesel. *Org. Biomol. Chem.* **2011**, *9*, 1908–1916.

(127) Boisset, A.; Jacquemin, J.; Anouti, M. Physical properties of a new deep eutectic solvent based on lithium bis[(trifluormethyl)-sulfonyl]imide and *N*-methylacetamide as superionic suitable electrolyte for lithium ion batteries and electric double layer capacitors. *Electrochim. Acta* **2013**, *102*, 120–126.

(128) Frisch, M. J.; Trucks, G. W.; Schlegel, H. B.; Scuseria, G. E.; Robb, M. A.; Cheeseman, J. R.; Scalmani, G.; Barone, V.; Mennucci, B.; Petersson, G. A.; Nakatsuji, H.; Caricato, M.; Li, X.; Hratchian, H. P.; Izmaylov, A. F.; Bloino, J.; Zheng, G.; Sonnenberg, J. L.; Hada, M.; Ehara, M.; Toyota, K.; Fukuda, R.; Hasegawa, J.; Ishida, M.; Nakajima, T.; Honda, Y.; Kitao, O.; Nakai, H.; Vreven, T.; Montgomery, J. A., Jr.; Peralta, J. E.; Ogliaro, F.; Bearpark, M.; Heyd, J. J.; Brothers, E.; Kudin, K. N.; Staroverov, V. N.; Kobayashi, R.; Normand, J.; Raghavachari, K.; Rendell, A.; Burant, J. C.; Iyengar, S. S.; Tomasi, J.; Cossi, M.; Rega, N.; Millam, J. M.; Klene, M.; Knox, J. E.; Cross, J. B.; Bakken, V.; Adamo, C.; Jaramillo, J.; Gomperts, R.; Stratmann, R. E.; Yazyev, O.; Austin, A. J.; Cammi, R.; Pomelli, C.; Ochterski, J. W.; Martin, R. L.; Morokuma, K.; Zakrzewski, V. G.; Voth, G. A.; Salvador, P.; Dannenberg, J. J.; Dapprich, S.; Daniels, A. D.; Farkas, Ö.; Foresman, J. B.; Ortiz, J. V.; Cioslowski, J.; Fox, D. J. *Gaussian 09*; Gaussian, Inc.: Wallingford, CT, 2009.

(129) *Materials Studio*; Accelrys: San Diego, CA, 2005.

(130) Earle, M. J.; Esperanca, J. M. S. S.; Gilea, M. A.; Canongia Lopes, J. N.; Rebelo, L. P. N.; Magee, J. W.; Seddon, K. R.; Widegren, J. A. The distillation and volatility of ionic liquids. *Nature* **2006**, *439*, 831–834.

(131) Esperanca, J. M. S. S.; Canongia Lopes, J. N.; Tariq, M.; Santos, L. M. N. B. F.; Magee, J. W.; Rebelo, L. P. N. Volatility of aprotic ionic liquids—a review. *J. Chem. Eng. Data* **2010**, *55*, 3–12.

(132) Hasan, N. H.; Said, M. R.; Leman, A. M. Health effect from volatile organic compounds and useful tools for future prevention: a review. *Int. J. Environ. Eng. Sci. Technol. Res.* **2013**, *1*, 28–36.

(133) Zielkiewicz, J. (Vapour + liquid) equilibrium measurements and correlation of the ternary mixture (*N*-methylacetamide + methanol + water) at the temperature 313.15 K. *J. Chem. Thermodyn.* **199**, *31*, 819–825.

(134) Wu, S. H.; Caparanga, A. R.; Leron, R. B.; Li, M. H. Vapor pressure of aqueous choline chloride-based deep eutectic solvents (ethaline, glyceline, maline and reline) at 30–70 °C. *Themochim. Acta* **2012**, *544*, 1–5.

(135) Valderrama, J. The state of the cubic equations of state. *Ind. Eng. Chem. Res.* **2003**, *42*, 1603–1618.

(136) D'Agostino, C.; Harris, R. C.; Abbott, A. P.; Gladden, L. F.; Mantle, M. D. Molecular motion and ion diffusion in choline chloride based deep eutectic solvents studied by ^{1}H pulsed gradient NMR spectroscopy. *Phys. Chem. Chem. Phys.* **2011**, *13*, 21383–21391.

(137) Mjalli, F.; Abdel-Jabbar, N. M. Acoustic investigation of choline chloride based ionic liquid analogs. *Fluid Phase Equilib.* **2014**, *381*, 71–76.

(138) Leron, R. B.; Li, M. H. High-pressure density measurements for choline chloride:urea deep eutectic solvent and its aqueous mixtures at T = (298.15 to 323.15) K and up to 50 MPa. *J. Chem. Thermodyn.* **2012**, *54*, 293–301.

(139) Yadav, A.; Pandey, S. Densities and viscosities of (choline chloride + urea) deep eutectic solvent and its aqueous mixtures in the temperature range 293.15 K to 363.15 K. *J. Chem. Eng. Data* **2014**, *59*, 2221–2229.

(140) Abbott, A.; Ahmed, E. I.; Harris, R. C.; Ryder, K. S. Evaluating water miscible deep eutectic solvents (DESs) and ionic liquids as potential lubricants. *Green Chem.* **2014**, *16*, 4156–4161.

(141) Leron, R. B.; Soriano, A. N.; Li, M. H. Densities and refractive indices of deep eutectic solvents (choline chloride + ethylene glycol or glycerol) and their aqueous mixtures at the temperature ranging from 298.15 to 333.15 K. *J. Taiwan Inst. Chem. Eng.* **2012**, *43*, 551–557.

(142) Yadav, A.; Trivedi, S.; Rai, R.; Pandey, S. Densities and dynamic viscosities of (choline chloride + glycerol) deep eutectic solvents and its aqueous mixtures in the temperature range (283.15–363.15) K. *Fluid Phase Equilib.* **2014**, *367*, 135–142.

(143) Leron, R.; Wong, R. S. H.; Li, M. H. Densities of a deep eutectic solvent based on choline chloride and glycerol and its aqueous mixtures at elevated pressures. *Fluid Phase Equilib.* **2012**, *335*, 32–38.

(144) Mjalli, F. S.; Vakili-Nezhaad, G.; Shahbaz, K.; AlNashef, I. M. Application of the Eötvos and Guggenheim empirical rules for predicting the density and surface tension of ionic liquids analogues. *Thermochim. Acta* **2014**, *575*, 40–44.

(145) Bahadori, L.; Chakrabarti, M. H.; Mjalli, F. S.; AlNashef, I. M.; Abdul-Naman, N. S.; Ali-Hashim, M. A. Physichochemical properties of ammonium-based deep eutectic solvents and their electrochemical evaluation using organometallic reference redox systems. *Electrochim. Acta* **2013**, *113*, 205–211.

(146) Yusof, R.; Abdulmalek, E.; Sirat, K.; Basyaruddin, M.; Rahman, M. A. Tetrabutylammonium bromide (TBABr)-based deep eutectic solvents (DESs) and their physical properties. *Molecules* **2014**, *19*, 8011–8026.

(147) Leron, R. B.; Li, M. H. High-pressure volumetric properties of choline chloride–ethylene glycol based deep eutectic solvent and its mixtures with water. *Thermochim. Acta* **2012**, *546*, 54–60.

(148) Dack, M. R. J. The importance of solvent internal pressure and cohesion to solution phenomena. *Chem. Soc. Rev.* **1975**, *4*, 211.

(149) Dávila, M. J.; Aparicio, S.; Alcalde, R.; García, B.; Leal, J. M. On the properties of 1-butyl-3-methylimidazolium octylsulfate ionic liquid. *Green Chem.* **2007**, *9*, 221–232.

(150) Aparicio, S.; Alcalde, R.; García, B.; Leal, J. M. High-pressure study of the methylsulfate and tosylate imidazolium ionic liquids. *J. Phys. Chem. B* **2009**, *113*, 5593–5606.

(151) Shahbaz, K.; Mjalli, F. S.; Hashim, M. A.; AlNashef, I. M. Prediction of deep eutectic solvents densities at different temperatures. *Thermochim. Acta* **2011**, *515*, 67–72.

(152) Siongco, K.; Leron, R. B.; Li, M. H. Densities, refractive indices, and viscosities of *N,N*-diethylethanolammonium chloride–glycerol or ethylene glycol deep eutectic solvents and their aqueous solutions. *J. Chem. Thermodyn.* **2013**, *65*, 65–72.

(153) Aparicio, S.; Atilhan, M. Water effect on CO$_2$ absorption for hydroxylammonium bases ionic liquids: a molecular dynamics study. *Chem. Phys.* **2012**, *400*, 118–125.

(154) Sun, W. C.; Wong, D. S. H.; Li, M. H. Effect of water on solubility of carbon dioxide in (aminomethanamide + 2-hydroxy-*N,N,N*-trimethylethanaminium chloride). *J. Chem. Eng. Data* **2009**, *54*, 1951–1955.

(155) Nanis, L.; Bockris, J. O. Self-diffusion. Heat of activation as a function of melting temperature. *J. Phys. Chem.* **1963**, *67*, 2865–2866.

(156) Emi, T.; Bockris, J. O. Semiempirical calculation of 3.7RT_m term in heat of activation for viscous flow of ionic liquid. *J. Phys. Chem.* **1970**, *74*, 159–163.

(157) Abbott, A. P.; Harris, R. C.; Ryder, K. S. Application of hole theory to define ionic liquids by their transport properties. *J. Phys. Chem. B* **2007**, *111*, 4910–4913.

(158) Bandrés, I.; Alcalde, R.; Lafuente, C.; Atilhan, M.; Aparicio, S. On the viscosity of pyridinium based ionic liquids: an experimental and computational study. *J. Phys. Chem. B* **2011**, *115*, 12499–12513.

(159) Shah, D.; Mjalli, F. S. Effect of water on the thermo-physical properties of reline: an experimental and molecular simulation based approach. *Phys. Chem. Chem. Phys.* **2014**, *16*, 23900–23907.

(160) Ghareh Bagh, F. S.; Shahbaz, K.; Mjalli, F. S.; AlNashef, I. M.; Hashim, M. A. Electrical conductivity of ammonium and phosphonium based deep eutectic solvents: measurements and artificial intelligence-based prediction. *Fluid Phase Equilib.* **2013**, *356*, 30–37.

(161) Tariq, M.; Freire, M. G.; Saramago, B.; Coutinho, J. A. P.; Canongia Lopes, J. N.; Rebelo, L. P. N. Surface tension of ionic liquids and ionic liquid solutions. *Chem. Soc. Rev.* **2012**, *41*, 829–868.

(162) Reichardt, C. Solvatochromic dyes as solvent polarity indicators. *Chem. Rev.* **1994**, *94*, 2319–2358.

(163) Kamlet, M. J.; Taft, R. W. The solvatochromic comparison method. I. The β-scale of solvent hydrogen-bond acceptor (HBA) basicities. *J. Am. Chem. Soc.* **1976**, *98*, 377–383.

(164) Reichardt, C. Polarity of ionic liquids determined empirically by means of solvatochromic pyridinium *N*-phenolate betaine dyes. *Green Chem.* **2005**, *7*, 339–351.

(165) Pandey, A.; Rai, R.; Pal, M.; Pandey, S. How polar are choline chloride-based deep eutectic solvents? *Phys. Chem. Chem. Phys.* **2014**, *16*, 1559–1568.

(166) Seki, S.; Tsuzuki, S.; Hayamizu, K.; Umebayashi, Y.; Serizawa, N.; Takei, K.; Miyahiro, H. Comprehensive refractive index property for room-temperature ionic liquids. *J. Chem. Eng. Data* **2012**, *57*, 2211–2216.

(167) Leron, R. B.; Li, M. H. Molar heat capacities of choline chloride-based deep eutectic solvents and their binary mixtures with water. *Thermochim. Acta* **2012**, *530*, 52–57.

(168) Siongco, K. R.; Leron, R. B.; Caparanga, A. R.; Li, M. H. Molar heat capacities and electrical conductivities of two ammonium-based deep eutectic solvents and their aqueous solutions. *Thermochim. Acta* **2013**, *566*, 50–56.

(169) Van Valkenburg, M. E.; Vaughn, R. L.; Williams, M.; Wilkes, J. S. Thermochemistry of ionic liquid heat-transfer fluids. *Thermochim. Acta* **2005**, *425*, 181–188.

(170) Rengstl, D.; Fischer, V.; Kunz, W. Low melting mixtures based on choline ionic liquids. *Phys. Chem. Chem. Phys.* **2014**, *16*, 22815–22822.

(171) Yue, D.; Jia, Y.; Yao, Y.; Sun, J.; Jing, Y. Structure and electrochemical behavior of ionic liquid analogue based on choline chloride and urea. *Electrochim. Acta* **2012**, *65*, 30–36.

(172) Dommert, F.; Wendler, K.; Berger, R.; Delle-Site, L. Force fields for studying the structure and dynamics of ionic liquids: a critical review of recent developments. *ChemPhysChem* **2012**, *13*, 1625–1637.

(173) Sun, H.; Li, Y.; Wu, X.; Li, G. Theoretical study on the structures and properties of mixtures of urea and choline chloride. *J. Mol. Model.* **2013**, *19*, 2433–2441.

(174) Perkins, S. L.; Painter, P.; Colina, C. M. Molecular dynamic simulations and vibrational analysis of an ionic liquid analogue. *J. Phys. Chem. B* **2013**, *117*, 10250–10260.

(175) Perkins, S. L.; Painter, P.; Colina, C. M. Experimental and computational studies of choline chloride-based deep eutectic solvents. *J. Chem. Eng. Data* **2014**, *59*, 3652–3662.

(176) Zhang, C.; Jia, Y.; Jing, Y.; Wang, H.; Hong, K. Main chemical species and molecular structure of deep eutectic solvent studied by experiments with DFT calculation: a case of choline chloride and magnesium chloride hexahydrate. *J. Mol. Model.* **2014**, *20*, 2374.

(177) Olajire, A. A. CO$_2$ capture and separation technologies for end-of-pipe applications—A review. *Energy* **2010**, *35*, 2610–2628.

(178) *IPCC Climate Change 2001: Impacts, Adaptation and Vulnerability. Contribution of Working Group II to the Third Assessment Report of the Intergovernmental Panel on Climate Change*; Cambridge University Press: Cambridge, U.K., 2001.

(179) Stewart, C.; Hessami, M. A. A study of methods of carbon dioxide capture and sequestration—The sustainability of a photo-

synthetic bioreactor approach. *Energy Convers. Manage.* **2005**, *46*, 403−420.

(180) *IPCC Special Report on Carbon Dioxide Capture and Storage*; Metz, B., Davidson, O., de Coninck, H., Loos, M., Meyer, L, Eds.; Cambridge University Press: Cambridge, U.K., 2005; available at http://www.ipcc.ch.

(181) *Natural Gas Issues and Trends 1998*; U.S. Energy Information Administration: Washington, D.C., 1998.

(182) Feron, P. H. M.; Hendriks, C. A. CO_2 capture process principles and costs. *Oil Gas Sci. Technol.* **2005**, *60*, 451−459.

(183) David, J. Economic evaluation of leading technology options for sequestration of carbon dioxide. M.S. Thesis, Massachusetts Institute of Technology, Cambridge, MA, 2000.

(184) Johnson, J. E.; Homme, A. C., Jr. Selexol solvent process reduces lean, high-CO_2 natural gas treating costs. *Energy Prog.* **1984**, *4*, 241−248.

(185) Weiss, H. Rectisol wash for purification of partial oxidation gases. *Gas Sep. Purif.* **1998**, 171−176.

(186) Aparicio, S.; Atilhan, M. Computational study of hexamethylguanidinium lactate ionic liquid: a candidate for natural gas sweetening. *Energy Fuels* **2010**, *24*, 4989−5001.

(187) Bates, E. D.; Mayton, R. D.; Ntai, I.; Davis, J. H. CO_2 capture by a task-specific ionic liquid. *J. Am. Chem. Soc.* **2002**, *124*, 926−927.

(188) Anthony, J. L.; Aki, S. N.; Maginn, E. J.; Brennecke, J. F. Feasibility of using ILs for carbon dioxide capture. *Int. J. Environ. Technol. Manage.* **2004**, *4*, 105−115.

(189) Pennline, H. W.; Luebke, D. R.; Jones, K. L.; Myers, C. R.; Morsi, B. L.; Heintz, Y. J.; Ilconich, J. B. Progress in carbon dioxide capture and separation research for gasification-based power generation point sources. *Fuel Process. Technol.* **2008**, *89*, 897−907.

(190) Bara, J. E.; Carlisle, T. K.; Gabriel, C. J.; Camper, D.; Finotello, A.; Gin, D. L.; Noble, R. D. Guide to CO_2 separations in imidazolium-based room-temperature ILs. *Ind. Eng. Chem. Res.* **2009**, *48*, 2739−2751.

(191) Lei, Z.; Dai, C.; Wang, W.; Chen, B. UNIFAC Model for Ionic Liquid—CO_2 Systems. *AIChE J.* **2014**, *60*, 716−729.

(192) Han, X.; Armstrong, D. W. ILs in separations. *Acc. Chem. Res.* **2007**, *40*, 1079−1086.

(193) Berthod, A.; Ruiz-Angel, M. J.; Carda-Broch, S. ILs in separation techniques. *J. Chromatogr., A* **2008**, *1184*, 6−18.

(194) Rogers, R. D. Reflections on ILs. *Nature* **2007**, *447*, 917−918.

(195) Karadas, F.; Köz, B.; Jacquemin, J.; Deniz, E.; Rooney, D.; Thompson, J.; Yavuz, C. T.; Khraisheh, M.; Aparicio, S.; Atihan, M. High pressure CO_2 absorption studies on imidazolium-based ionic liquids: Experimental and simulation approaches. *Fluid Phase Equilib.* **2013**, *351*, 74−86.

(196) Ng, S.; Atilhan, M.; Karadas, F.; Jacquemin, J.; Thompson, J.; Rooney, D.; Khraisheh, M. Applications of ionic liquids in gas processing. In *Proceedings of the 3rd Gas Processing Symposium*; Benyahia, A. A., Ed.; Elsevier: Oxford, U.K., 2012; Vol. 3, pp 133−138.

(197) *Recent Advances in Post-Combustion CO_2 Capture Chemistry*; Attalla Moetaz, I., Ed.; ACS Symposium Series, Vol. *1097*; American Chemical Society: Washington, DC, 2012.

(198) Cassidy, C. G.; Mirjafari, A.; Mobarrez, N.; Strickland, K. J.; O'Brien, R. A.; Davis, J. H. Ionic liquids of superior thermal stability. *Chem. Commun.* **2013**, *49*, 7590−7592.

(199) Cadena, C.; Anthony, J. L.; Shah, J. K.; Morrow, T. I.; Brennecke, J. F.; Maginn, E. J. Why is CO_2 so soluble in imidazolium-based ionic liquids? *J. Am. Chem. Soc.* **2004**, *126*, 5300−5308.

(200) Torralba-Calleja, E.; Skinner, J.; Gutiérrez-Tauste, D. CO_2 capture in ionic liquids: A review of solubilities and experimental methods. *J. Chem.* **2013**, DOI: 10.1155/2013/473584.

(201) Bara, J. E.; Gabriel, C. J.; Lessman, S.; Carlisle, T. K.; Finotello, A.; Gin, D. L.; Noble, R. D. Enhanced CO_2 separation selectivity in oligo(ethylene glycol) functionalized room-temperature ionic liquids. *Ind. Eng. Chem. Res.* **2007**, *46*, 5380−5386.

(202) Blanchard, L. A.; Hancu, D.; Beckmann, E. J.; Brennecke, J. F. Green processing using ionic liquids and CO_2. *Nature* **1999**, *399*, 28−29.

(203) Anderson, J. L.; Dixon, J. K.; Brennecke, J. F. Solubility of CO_2, CH_4, C_2H_6, C_2H_4, O_2, and N_2 in 1-hexyl-3-methylpyridinium bis(trifluoromethylsulfonyl)imide: comparison to other ionic liquids. *Acc. Chem. Res.* **2007**, *40*, 1208−1216.

(204) Anthony, J. L.; Maginn, E. J.; Brennecke, J. F. Solubilities and thermodynamic properties of gases in the ionic liquid 1-*n*-butyl-3-methylimidazolium hexafluorophosphate. *J. Phys. Chem. B* **2002**, *106*, 7315−7320.

(205) Baltus, R. E.; Culbertson, B. H.; Dai, S.; Luo, H.; DePaoli, D. W. Low-pressure solubility of carbon dioxide in room-temperature ionic liquids measured with a quartz crystal microbalance. *J. Phys. Chem. B* **2004**, *108*, 721−727.

(206) Hwang, B. J.; Park, S. W.; Park, D. W.; Oh, K. J.; Kim, S. S. Absorption of carbon dioxide into ionic liquid of 2-hydroxyethylammonium lactate. *Sep. Sci. Technol.* **2009**, *44*, 1574−1589.

(207) Jacquemin, J.; Husson, P.; Majer, V.; Costa Gomes, M. F. Low-pressure solubilities and thermodynamics of solvation of eight gases in 1-butyl-3-methylimidazolium hexafluorophosphate. *Fluid Phase Equilib.* **2006**, *240*, 87−95.

(208) Pérez-Salado Kamps, A.; Tuma, D.; Xia, J.; Maurer, G. Solubility of CO_2 in the Ionic Liquid [bmim][PF_6]. *J. Chem. Eng. Data* **2003**, *48*, 746−749.

(209) Kumełan, J.; Tuma, D.; Maurer, G. Solubility of CO_2 in the ionic liquids [bmim][CH_3SO_4] and [bmim][PF_6]. *J. Chem. Eng. Data* **2006**, *51*, 1802−1807.

(210) Shiflett, M. B.; Yokozeki, A. Solubilities and diffusivities of carbon dioxide in ionic liquids: [bmim][PF_6] and [bmim][BF_4]. *Ind. Eng. Chem. Res.* **2005**, *44*, 4453−4464.

(211) Soriano, A. N.; Doma, B. T., Jr.; Li, M. H. Carbon dioxide solubility in 1-ethyl-3-methylimidazolium trifluoromethanesulfonate. *J. Chem. Thermodyn.* **2009**, *41*, 525−529.

(212) Zhang, X.; Huo, F.; Liu, Z.; Wang, W.; Shi, W.; Maginn, E. J. Absorption of CO_2 in the ionic liquid 1-*n*-hexyl-3-methylimidazolium tris(pentafluoroethyl)trifluorophosphate ([hmim][FEP]): a molecular view by computer simulations. *J. Phys. Chem. B* **2009**, *113*, 7591−7598.

(213) Aki, S. N. V. K.; Mellein, B. R.; Saurer, E. M.; Brennecke, J. F. High-pressure phase behavior of carbon dioxide with imidazolium-based ionic liquids. *J. Phys. Chem. B* **2004**, *108*, 20355−20365.

(214) Muldoon, M. J.; Aki, S. N. V. K.; Anderson, J. L.; Dixon, J. K.; Brennecke, J. F. Improving carbon dioxide solubility in ionic liquids. *J. Phys. Chem. B* **2007**, *111*, 9001−9009.

(215) Luo, X. Y.; Ding, F.; Lin, W. J.; Qi, Y. Q.; Li, H. R.; Wang, C. M. Efficient and energy-saving CO_2 capture through the entropic effect induced by the intermolecular hydrogen bonding in anion-functionalized ionic liquids. *J. Phys. Chem. Lett.* **2014**, *5*, 381−386.

(216) Carvalho, P. J.; Coutinho, J. A. P. On the nonideality of CO_2 solutions in ionic liquids and other low volatile solvents. *J. Phys. Chem. Lett.* **2010**, *1*, 774−780.

(217) Ramdin, M.; Amplianitis, A.; Bazhenov, S.; Volkov, A.; Volkov, V.; Vlugt, T.; de Loos, T. W. Solubility of CO_2 and CH_4 in ionic liquids: ideal CO_2/CH_4 selectivity. *Ind. Eng. Chem. Res.* **2014**, *53*, 15427−15435.

(218) Supasitmongkol, S.; Styring, P. High CO_2 solubility in ionic liquids and a tetraalkylammonium-based poly(ionic liquid). *Energy Environ. Sci.* **2010**, *3*, 1961−1972.

(219) Faúndez, C. A.; Díaz-Valdés, J. F.; Valderrama, J. O. Testing solubility data of H_2S and SO_2 in ionic liquids for sulfur-removal processes. *Fluid Phase Equilib.* **2014**, *375*, 152−160.

(220) Anderson, J. L.; Dixon, J. K.; Maginn, E. J.; Brennecke, J. F. Measurement of SO_2 solubility in ionic liquids. *J. Phys. Chem. B* **2006**, *110*, 15059−15062.

(221) Jalili, A. M.; Rahmati-Rostami, M.; Ghotbi, C.; Hosseini-Jenab, M.; Ahmadi, A. N. Solubility of H_2S in ionic liquids [hmim][PF_6], [hmim][BF_4], and [hmim][Tf_2N]. *J. Chem. Thermodyn.* **2009**, *41*, 1052−1055.

(222) Wu, W.; Han, B.; Gao, H.; Liu, Z.; Jiang, T.; Huang, J. Desulfurization of flue gas: SO_2 absorption by an ionic liquid. *Angew. Chem., Int. Ed.* **2004**, *43*, 2415−2417.

(223) Yokozeki, A.; Shiflett, M. B. Separation of carbon dioxide and sulfur dioxide gases using room-temperature ionic liquid [hmim]-[Tf$_2$N]. *Energy Fuels* **2009**, *23*, 4701−4708.

(224) Tang, S.; Baker, G. A.; Zhao, H. Ether- and alcohol-functionalized task-specific ionic liquids: attractive properties and applications. *Chem. Soc. Rev.* **2012**, *41*, 4030−4066.

(225) Sze, L. L.; Pandey, S.; Ravula, S.; Pandey, S.; Zhao, H.; Baker, G. A.; Baker, S. N. Ternary deep eutectic solvents tasked for carbon dioxide capture. *ACS Sustainable Chem. Eng.* **2014**, *2*, 2117−2123.

(226) Leron, R. B.; Caparanga, A.; Li, M. H. Carbon dioxide solubility in a deep eutectic solvent based on choline chloride and urea at T = 303.15−343.15 K and moderate pressures. *J. Taiwan Inst. Chem. Eng.* **2013**, *44*, 879−885.

(227) Leron, R. B.; Li, M. H. Solubility of carbon dioxide in a choline chloride−ethylene glycol based deep eutectic solvent. *Thermochim. Acta* **2013**, *551*, 14−19.

(228) Ali, E.; Hadj-Kali, M.; Mulyono, S.; AlNashef, I.; Fakeeha, A.; Mjalli, F.; Hayyan, A. Solubility of CO$_2$ in deep eutectic solvents: experiments and modelling using the Peng−Robinson equation of state. *Chem. Eng. Res. Des.* **2014**, *92*, 1898−1908.

(229) Soriano, A. N.; Doma, B. T.; Li, M. H. Solubility of carbon dioxide in 1-ethyl-3-methylimidazolium tetrafluoroborate. *J. Chem. Eng. Data* **2008**, *53*, 2550−2555.

(230) Li, G.; Deng, D.; Chen, Y.; Shan, H.; Ai, N. Solubilities and thermodynamic properties of CO$_2$ in choline-chloride based deep eutectic solvents. *J. Chem. Thermodyn.* **2014**, *75*, 58−62.

(231) Yang, D.; Hou, M.; Ning, H.; Zhang, J.; Ma, J.; Yang, G.; Han, B. Efficient SO$_2$ absorption by renewable choline chloride−glycerol deep eutectic solvents. *Green Chem.* **2013**, *15*, 2261−2265.

(232) Huang, K.; Lu, J. F.; Wu, Y. T.; Hu, X. B.; Zhang, Z. B. Absorption of SO$_2$ in aqueous solutions of mixed hydroxylammonium dicarboxylate ionic liquids. *Chem. Eng. J.* **2013**, *215−216*, 36−44.

(233) Liu, B.; Wei, F.; Zhao, J.; Wang, Y. Characterization of amide−thiocyanates eutectic ionic liquids and their application in SO$_2$ absorption. *RSC Adv.* **2013**, *3*, 2470−2476.

(234) Yang, Z.-Z.; Yang, Z. Z.; He, L. N.; Zhao, Y. N.; Li, B.; Yu, B. CO$_2$ capture and activation by superbase/polyethylene glycol and its subsequent conversion. *Energy Environ. Sci.* **2011**, *4*, 3971−3975.

(235) Wang, C.; Mahurin, S. M.; Luo, H.; Baker, G. A.; Li, H.; Dai, S. Reversible and robust CO$_2$ capture by equimolar task-specific ionic liquid−superbase mixtures. *Green Chem.* **2010**, *12*, 870−874.

(236) Wang, G. N.; Dai, Y.; Hu, X. B.; Xiao, F.; Wu, Y. T.; Zhang, Z. B.; Zhou, Z. Novel ionic liquid analogs formed by triethylbutylammonium carboxylate−water mixtures for CO$_2$ absorption. *J. Mol. Liq.* **2012**, *168*, 17−20.

(237) Leron, R. B.; Li, M. H. Solubility of carbon dioxide in a eutectic mixture of choline chloride and glycerol at moderate pressures. *J. Chem. Thermodyn.* **2013**, *57*, 131−136.

(238) Guo, B.; Duan, E.; Ren, A.; Wang, Y.; Liu, H. Solubility of SO$_2$ in caprolactam tetrabutyl ammonium bromide ionic liquids. *J. Chem. Eng. Data* **2009**, *55*, 1398−1401.

(239) Duan, E.; Guo, B.; Zhang, M.; Guan, Y.; Sun, H.; Han, J. Efficient capture of SO$_2$ by a binary mixture of caprolactam tetrabutyl ammonium bromide ionic liquid and water. *J. Hazard. Mater.* **2011**, *194*, 48−52.

(240) Liu, B.; Zhao, J.; Wei, F. Characterization of caprolactam based eutectic ionic liquids and their application in SO$_2$ absorption. *J. Mol. Liq.* **2013**, *180*, 19−25.

(241) Chen, Y.; Ai, N.; Li, G.; Shan, H.; Cui, Y.; Deng, D. Solubilities of carbon dioxide in eutectic mixtures of choline chloride and dihydric alcohols. *J. Chem. Eng. Data* **2014**, *59*, 1247−1253.

(242) Francisco, M.; van der Bruinhorst, A.; Zubeir, L. F.; Peters, C. J.; Kroon, M. C. A new low transition temperature mixture (LTTM) formed by choline chloride + lactic acid: characterization as solvent for CO$_2$ capture. *Fluid Phase Equilib.* **2013**, *340*, 77−84.

(243) Li, X.; Hou, M.; Han, B.; Wang, X.; Zou, L. Solubility of CO$_2$ in a choline chloride + urea eutectic mixture. *J. Chem. Eng. Data* **2008**, *53*, 548−550.

(244) Hsu, Y.-H.; Leron, R. B.; Li, M. H. Solubility of carbon dioxide in aqueous mixtures of (reline + monoethanolamine) at T = (313.2 to 353.2) K. *J. Chem. Thermodyn.* **2014**, *72*, 94−99.

(245) Schubert, T. Electrodeposition of Metals. In *Electrodeposition from Ionic Liquids*; Endres, F., MacFarlane, D., Abbott, A., Eds.; Wiley-VCH: Weinheim, Germany, 2008; pp 83−123.

(246) Abbott, A. P.; McKenzie, K. J. Application of ionic liquids to the electrodeposition of metals. *Phys. Chem. Chem. Phys.* **2006**, *8*, 4265−4279.

(247) Abbott, A. P.; El-Ttaib, K.; Frisch, G.; Ryder, K. S.; Weston, D. The electrodeposition of silver composites using deep eutectic solvents. *Phys. Chem. Chem. Phys.* **2012**, *14*, 2443−2449.

(248) Abbott, A. P.; El-Ttaib, K.; Frisch, G.; McKenzie, K. J.; Ryder, K. S. Electrodeposition of copper composites from deep eutectic solvents based on choline chloride. *Phys. Chem. Chem. Phys.* **2009**, *11*, 4269−4277.

(249) Zhao, H.; Baker, G. A.; Holmes, S. Protease activation in glycerol-based deep eutectic solvents. *J. Mol. Catal. B: Enzym.* **2011**, *72*, 163−167.

(250) Lindberg, D.; Revenga, M. D. L. F.; Widersten, M. Deep eutectic solvents (DESs) are viable cosolvents for enzyme-catalyzed epoxide hydrolysis. *J. Biotechnol.* **2010**, *147*, 169−171.

(251) Zhao, H.; Zhang, C.; Crittle, T. D. Choline-based deep eutectic solvents for enzymatic preparation of biodiesel from soybean oil. *J. Mol. Catal. B: Enzym.* **2013**, *85*, 243−247.

(252) Abbott, A. P.; Cullis, P. M.; Gibson, M. J.; Harris, R. C.; Raven, E. Extraction of glycerol from biodiesel into a eutectic based ionic liquid. *Green Chem.* **2007**, *9*, 868−872.

(253) Wang, C.; Luo, H.; Luo, X.; Li, H.; Dai, S. Equimolar CO$_2$ capture by imidazolium-based ionic liquids and superbase systems. *Green Chem.* **2010**, *12*, 2019−2023.

(254) Wang, C.; Luo, X.; Luo, H.; Jiang, D.; Li, H.; Dai, S. Tuning the basicity of ionic liquids for equimolar CO$_2$ capture. *Angew. Chem., Int. Ed.* **2011**, *50*, 4918−4922.

(255) Yang, Z.-Z.; Zhao, Y. N.; He, L. N. CO$_2$ chemistry: task-specific ionic liquids for CO$_2$ capture/activation and subsequent conversion. *RSC Adv.* **2011**, *1*, 545−567.

(256) Zhang, S.; Chen, Y.; Ren, R. X. F.; Zhang, Y.; Zhang, J.; Zhang, X. Solubility of CO$_2$ in sulfonate ionic liquids at high pressure. *J. Chem. Eng. Data* **2005**, *50*, 230−233.

(257) Galán Sánchez, L. M.; Meindersma, G. W.; de Haan, A. B. Solvent properties of functionalized ionic liquids for CO$_2$ absorption. *Chem. Eng. Res. Des.* **2007**, *85*, 31−39.

(258) Introduction: The Sulfur Problem. In *The Sulfur Problem: Cleaning Up Industrial Feedstocks*; Stirling, D., Clark, J. H., Eds.; Royal Society of Chemistry: Cambridge, U.K., 2000; pp 1−9.

(259) Gutiérrez Ortiz, F. J.; Vidal, F.; Ollero, P.; Salvador, L.; Cortes, V. Pilot-plant technical assessment of wet flue gas desulfurization using limestone. *Ind. Eng. Chem. Res.* **2006**, *45*, 1466−1477.

(260) Hansen, B. B.; Kiil, S.; Johnson, J. E.; Sonder, K. B. Foaming in wet flue gas desulfurization plants: the influence of particles, electrolytes, and buffers. *Ind. Eng. Chem. Res.* **2008**, *47*, 3239−3246.

(261) Matsushima, N.; Li, Y.; Nishioka, M.; Sadakata, M. Novel dry-desulfurization process using Ca(OH)$_2$/fly ash sorbent in a circulating fluidized bed. *Environ. Sci. Technol.* **2004**, *38*, 6867−6874.

(262) Tian, S.; Hou, Y.; Wu, W.; Ren, S.; Zhang, C. Absorption of SO$_2$ by thermal-stable functional ionic liquids with lactate anion. *RSC Adv.* **2013**, *3*, 3572−3577.

(263) Wang, C.; Zheng, J.; Cui, G.; Luo, X.; Guo, Y.; Li, H. Highly efficient SO$_2$ capture through tuning the interaction between anion-functionalized ionic liquids and SO$_2$. *Chem. Commun.* **2013**, *49*, 1166−1168.

(264) Wang, C.; Cui, G.; Luo, X.; Xu, Y.; Li, H.; Dai, S. Highly efficient and reversible SO$_2$ capture by tunable azole-based ionic liquids through multiple-site chemical absorption. *J. Am. Chem. Soc.* **2011**, *133*, 11916−11919.

(265) Shannon, M. S.; Irvin, A. C.; Liu, H.; Moon, J. D.; Hindman, M. S.; Turner, C. H.; Bara, J. E. Chemical and physical absorption of

SO$_2$ by N-functionalized imidazoles: experimental results and molecular-level insight. *Ind. Eng. Chem. Res.* **2015**, *54*, 462−471.

(266) Li, X.; Zhang, L.; Zheng, Y.; Zheng, C. SO$_2$ absorption performance enhancement by ionic liquid supported on mesoporous molecular sieve. *Energy Fuels* **2015**, *29*, 942−953.

(267) Wang, J.; Zeng, S.; Bai, L.; Gao, H.; Zhang, X.; Zhang, S. Novel ether-functionalized pyridinium chloride ionic liquids for efficient SO$_2$ capture. *Ind. Eng. Chem. Res.* **2014**, *53*, 16832−16839.